

New pedotransfer approaches to predict soil bulk density using WoSIS soil data and environmental covariates in Mediterranean agro-ecosystems

Calogero Schillaci¹, Alessia Perego^{1*}, Elena Valkama², Michael Märker³, Sergio Saia⁴, Fabio Veronesi⁵, Aldo Lipani⁶, Luigi Lombardo⁷, Tommaso Tadiello¹, Hannes A. Gamper⁸, Luigi Tedone⁹, Cami Moss¹⁰, Elena Pareja-Serrano¹¹, Gabriele Amato¹², Kersten Kühl¹³, Claudia Damatirca¹⁴, Alessia Cogato¹⁵, Nada Mzid¹⁶, Rasu Eeswaran¹⁷, Marya Rebelo¹⁸, Giorgio Sperandio¹⁹, Alberto Bosino³, Margherita Bufalini²⁰, Tülay Tunçay²¹, Jianqi Ding²², Marco Fiorentini²³, Guadalupe Tiscornia²⁴, Sarah Conradt²⁵, Marco Botta¹, Marco Acutis¹

1 Department of Agricultural and Environmental Science, University of Milan, Via Celoria 2 Milan, Italy
2 Natural Resources Institute Finland (Luke), Bioeconomy and Environment, FI-31600, Tietotie 4, Jokioinen, Finland
3 Department of Earth and Environmental Sciences, University of Pavia, Via Ferrata, 1, 27100 Pavia, Italy
4 Department of Veterinary Sciences, University of Pisa, Via delle Piagge 2, Pisa 56129, Italy
5 Water Research Centre Limited, Frankland Road, Blagrove, Swindon, Wiltshire, SN56 8YF, England
6 Department of Civil, Environmental and Geomatic Engineering, University College London (UCL), Gower Street, London, UK
7 Faculty of Geo-Information Science and Earth Observation (ITC), University of Twente, PO Box 217, Enschede, AE 7500, The Netherlands
8 Faculty of Science and Technology, Free University of Bozen, Piazza Università, 5 39100 Bolzano, Italy
9 Department of Agricultural and Environmental Science, University of Bari Aldo Moro, Via Amendola 165/A-, 70126 Bari, Italy
10 Department of Population Health, London School of Hygiene & Tropical Medicine, London WC1E 7HT, UK
11 Remote Sensing and GIS Group, Instituto de Desarrollo Regional, University of Castilla-La Mancha, 02071 Campus of Albacete, Spain
12 IFAC CNR, Via Madonna del Piano, 10, 50019 Sesto Fiorentino, Florence, Italy
13 Department of Geography Ludwig-Maximilians-University of Munich, Germany
14 Department of Agricultural, Forest and Food Sciences, University of Torino, largo Braccini 2, 10095 Grugliasco, Italy
15 Department of Land, Environmental, Agriculture and Forestry, University of Padova, 35020 Legnaro, Italy
16 Department of Sciences and Technology for Agriculture, Forest, Environment and Energy, DAFNE, Università della Tuscia, Viterbo, Italy
17 Department of Plant, Soil and Microbial Sciences, Michigan State University, East Lansing, MI48824, USA
18 Department of Agriculture, Food and Environment, University of Pisa, via del Borghetto 80, 56124 Pisa, Italy
19 Dipartimento di Medicina Molecolare e Traslazionale, Università di Brescia, Viale Europa, 11, 25123 Brescia, Italy
20 University of Camerino, School of Science and Technology-Geology Division, Via Gentile III da Varano, Camerino 62032, Italy
21 Soil Fertilizer and Water Resources Central Research Institute, Ankara-Turkey
22 Department of Biological and Ecological Sciences DEB, Università della Tuscia, Viterbo, Italy
23 Department of Agricultural, Food and Environmental Sciences (D3A), Marche Polytechnic University, Ancona, Italy
24 Instituto Nacional de Investigación Agropecuaria (INIA). Unidad Agroclima y Sistemas de Información (GRAS). Ruta 48 KM10, Canelones 90200, Uruguay.
25 SCOR SE, Zurich Branch, Switzerland

*corresponding author

Keywords: Agriculture, bulk density, pedotransfer functions, PTFs, soil carbon, soil texture

Highlights

- Three PTFs were developed to calculate bulk density of arable top- and subsoil
- WoSIS, WorldClim, and topographic data of the Mediterranean Basin were used
- Model transferability of the three new PTFs was validated with external dataset
- Topsoil ANN-PTF had R^2 of 0.89 in training and 0.45 in model transferability
- ANN-PTF outperformed the commonly employed PTF by Manrique and Jones

Abstract

For the estimation of the soil organic carbon stocks, bulk density (BD) is a fundamental parameter but measured data are usually not available especially when dealing with legacy soil data. It is possible to estimate BD by applying pedotransfer function (PTF). We applied different estimation methods with the

52 aim to define a suitable PTF for BD of arable land for the Mediterranean Basin, which has peculiar climate
53 features that may influence the soil carbon sequestration. To improve the existing BD estimation methods,
54 we used a set of public climatic and topographic data along with the soil texture and organic carbon data.
55 The present work consisted of the following steps: i) development of three PTFs models separately for top
56 (0-0.4 m) and subsoil (0.4-1.2 m), ii) a 10-fold cross-validation, iii) model transferability using an external
57 dataset derived from published data.

58 The development of the new PTFs was based on the training dataset consisting of World Soil Information
59 Service (WoSIS) soil profile data, climatic data from WorldClim at 1 km spatial resolution and Shuttle
60 Radar Topography Mission (SRTM) digital elevation model at 30 m spatial resolution.

61 The three PTFs models were developed using: Multiple Linear Regression stepwise (MLR-S), Multiple
62 Linear Regression backward stepwise (MLR-BS), and Artificial Neural Network (ANN).

63 The predictions of the newly developed PTFs were compared with the BD calculated using the PTF
64 proposed by Manrique and Jones (MJ) and the modelled BD derived from the global SoilGrids dataset.

65 For the topsoil training dataset (N=129), MLR-S, MLR-BS and ANN had a R^2 0.35, 0.58 and 0.86,
66 respectively. For the model transferability, the three PTFs applied to the external topsoil dataset (N=59),
67 achieved R^2 values of 0.06, 0.03 and 0.41. For the subsoil training dataset (N=180), MLR-S, MLR-BS and
68 ANN the R^2 values were 0.36, 0.46 and 0.83, respectively. When applied to the external subsoil dataset
69 (N=29), the R^2 values were 0.05, 0.06 and 0.41. The cross-validation for both top and subsoil dataset,
70 resulted in an intermediate performance compared to calibration and validation with the external dataset.
71 The new ANN PTF outperformed MLR-S, MLR-BS, MJ and SoilGrids approaches for estimating BD.
72 Further improvements may be achieved by additionally considering the time of sampling, agricultural soil
73 management and cultivation practices in predictive models.

74 **1. Introduction**

75 Soil bulk density (BD) is directly linked to soil functionality including mechanical support of crop
76 plants, circulation of soil solution, and soil aeration (Håkansson and Lipiec, 2000). Relatively high

77 values of BD indicate soil compaction which may lead to reduced water infiltration especially in
78 agricultural land, where it can hamper the growth of crop root systems (Colombi et al., 2018). Soil
79 BD is calculated as the dry weight of soil divided by its volume. Volumes include soil particle
80 volume and pore space between soil particles. Soil BD is typically expressed in g cm^{-3} or Mg m^{-3}
81 (SI). Along with soil organic carbon (SOC) concentrations, soil BD is necessary to calculate SOC
82 stocks (Minasny et al., 2013) and to assess carbon sequestration (Tao et al., 2019). Many soil
83 physical and chemical properties are expressed on a volumetric basis and in particular the
84 estimation of soil biological properties depend on BD estimates (Tejada et al., 2009). In arable
85 lands, tillage and other management practices cause high variation of BD during the year.
86 Scientists have tried to infer BD from soil properties that are routinely measured such as textural
87 information and organic carbon content (Acutis and Donatelli, 2003; Alvarez-Acosta et al., 2012;
88 Pachepsky et al., 1996; Van Looy et al., 2017). The functions enabling the estimation of a given
89 soil property (e.g. BD) from other variables, routinely obtained through laboratory measurement,
90 are called pedotransfer functions (PTF) (Bouma, 1989; Patil and Singh, 2016). PTFs have been
91 used at global scale to estimate the soil water retention, soil particle size, soil BD and SOC stock
92 (Batjes and Dijkshoorn, 1999; Rawls, 1983; Rawls and Pachepsky, 2002; Reynolds et al., 2000;
93 Saxton et al., 1986). At this scale, soil BD models had limited predictive ability (Rawls, 1983;
94 Tietje and Tapkenhinrichs, 1993). Unfortunately, PTFs are not able to fully replace direct
95 measurements, as highlighted in a recent publication which compared >50 PTFs using high
96 resolution geodata in at district scale (Nasta et al., 2020; Xiangsheng et al., 2016). PTF are also
97 frequently chosen at district scales after a sensitivity analysis (Basile et al., 2019).

98 Accurate models are of high interest for land management and policy-making especially where
99 sparse data are available.

100 Today, BD estimates are used to quantify and model the SOC stocks in top- and subsoil at regional
101 and global scales (Valkama et al., 2020). For example, Sun et al. (2020) recently used PTF in a
102 meta-analysis to assess the effect of conservation agriculture on carbon stocks but did not provide
103 an assessment of the PTF function performance.

104 One of the first attempts to estimate BD was made by Manrique and Jones (1991) who proposed
105 a PTF based on SOC alone ($BD=1.660-0.318 \cdot SOC^{0.5}$) for all soil types. Since then, other PTFs
106 for BD estimation have been developed based on the fine earth fractions and SOC, which is
107 important to BD due to its effect on the ratio between soil macro- and micropores (Martín et al.,
108 2017; Throop et al., 2012). Furthermore, many other functions have been proposed to describe
109 regional (Akpa et al. 2016; Chagas et al., 2016; Chen et al., 2018; Makovníková et al., 2017;
110 Montzka et al., 2017; Ramcharan et al., 2017; Román Dobarco et al., 2019; Wösten et al., 2013,
111 1999) and local conditions (Benites et al., 2007; De Vos et al., 2005; Picciafuoco et al., 2019;
112 Sevastas et al., 2018) and to predict BD in different soil horizons (Hollis et al., 2012; Reidy et al.,
113 2016; Sequeira et al., 2014).

114 In the absence of measured soil data, the availability of new topographic data such as digital
115 elevation models and morphometric indices has also improved soil assessment (Lombardo et al.
116 2018, Schillaci et al., 2017a, b, 2019; Veronesi and Schillaci, 2019) and in particular to develop
117 PTF (Leij et al., 2004; Romano and Chirico, 2004). Other geodata (e.g., climate, satellite-derived,
118 land cover) correlated with BD have also been used to improve estimates (Aitkenhead and Coull,
119 2020). Various researchers have recently developed new methods to estimate BD.

120 Bondi et al., (2018) estimated BD for peat soils using soil visual assessment, and decision trees
121 achieving similar performances, with around 0.6 explained variance. Premrov et al., (2018)

122 achieved similar performances (R^2 from 0.4 to 0.6) using optimal power-transformation of
123 measured physical and chemical soil parameters.

124 Chen et al. (2018) formalized an analytical protocol to test the PTF prediction at regional scales
125 in France by building a Boosted Regression Tree (BRT) model to obtain reliable predictions (R^2
126 0.7) , and also applied the advanced deep learning modelling framework for the evaluation of in
127 situ spectral measurement of SOC with in situ vis-NIR spectroscopy in southeastern Tibet (Chen
128 et al., 2020) achieving ($R^2 = 0.92$). Rodríguez-Lado et al. (2015) used a dataset consisting of 115
129 topsoil observations in a catchment of approximately 100 km² to map soil BD and compared three
130 methods: Stepwise Multiple Linear Regression (MLR-S), Random Forest (RF) and Artificial
131 Neural Networks (ANN). In this procedure, RF and ANN appeared the most suitable approaches
132 to predict the measured data, producing R^2 of 0.90 and 0.86, respectively. These results suggest
133 that soil samples remain essential to obtain good estimates, and that PTFs derived from data
134 collected in given locations can fail to give accurate estimates when applied elsewhere (Akpa et
135 al., 2016). PTFs modelling is a relatively new subject and many important steps have been carried
136 out recently (Chen et al., 2018; Sevastas et al., 2018). To extract all the contributions on soil BD,
137 simple query can be used to gather publications from SCOPUS and Web of Knowledge (Schillaci
138 et al., 2018). Out of this search the most used approach for the BD estimation with PTFs is multiple
139 linear regression (60%) followed by ANN (20 %), therefore these two approaches are investigated
140 here.

141 At present the available PTF models offer wide predictive ranges and none are specifically
142 developed for the Mediterranean area. The aim of this study was to develop new regionally-
143 specific BD prediction models using data gathered from the literature on soil texture, SOC,
144 topography and climate in Mediterranean agro-ecosystems. As well as providing a modelling

145 framework that can be applied in each environmental setting. In the Mediterranean basin area, soil
146 organic matter mineralization is boosted by high-temperature conditions (Álvaro-Fuentes and
147 Paustian, 2011), in which rainfall has a peculiar pattern (availability during a short season vs long
148 dry period). Moreover, the agricultural systems are conventionally plough-based (Mazzoncini et
149 al., 2011) causing soil compaction and reduced SOC stocks.

150 **2. Material and Methods**

151 The study was conceptualized during the first annual summer school module “Statistical Analysis
152 of Spatial Data in Agro-Environmental Research”, organized in cooperation with Lake Como
153 Advanced School (<https://sdae.lakecomoschool.org/>), and held from August 26-30, 2019. As a
154 practical teaching activity, soil legacy data and topographic datasets were compiled to develop a
155 PTF. The school participants were mainly PhD students and early career researchers. The present
156 work was carried out after the school as a collaboration between students and teachers.

157 **2.1 Operational procedures**

158
159 Study work streams included PTF development using training datasets from public databases, and
160 PTF validation using an independent validation dataset compiled from systematic review of the
161 literature (Table 1 and Fig. 1). In the training step, we defined three PTFs – two based on statistical
162 approaches and one based on ANN. In the validation step, we applied the three newly-defined
163 PTFs to an external dataset. We then compared the performances of the three PTFs and
164 benchmarked them against those of the MJ PTF and SoilGrids estimates (see below). The training
165 and validation datasets were each split into topsoil and subsoil to infer separate PTFs.

166

168 *Table 1. Study overview and workflow to develop pedotransfer functions (PTF) to infer soil bulk*
 169 *density (BD) in top- (0-0.4m) and subsoil (0.4-1.2) of arable fields in the Mediterranean*

	New PTFs to estimate BD			Reference PTF and BD data	
<i>Study stage</i>	MLR-S: stepwise regression	MLR- BS: backward + stepwise regression	ANN: artificial neural network	Manrique-Jones (1991): PTF function for estimating BD	SoilGrids: estimated BD values derived from WoSIS data
<i>Training</i>	Developed database* + climatic data	using + topographic	WoSIS +		
<i>Validation and Benchmarking</i>	Applied on external topographic + climatic data	database** + climatic data		Applied on external database**	Available at 250 m grid

170 * WoSIS database: measured data of bulk density (BD, Mg m⁻³), soil organic carbon (%), sand

171 ** newly compiled database of soil bulk density, organic carbon, sand, silt and clay measurements

172 of studies from the Mediterranean

Training dataset	Validation dataset
<p style="text-align: center;">Source</p> <p>WoSIS open database of geo-referenced soil profiles sampling with soil properties: Bulk density, Texture, SOC, Rock fragment content, sample depth</p>	<p style="text-align: center;">Source</p> <p>Soil properties of studies carried out in the Mediterranean: Bulk density, Texture, SOC, Rock fragment content, sampling depth</p>
<p style="text-align: center;">Extraction</p> <p>WoSIS shapefile with geo-referenced study locations with soil physical and chemical soil data</p>	<p style="text-align: center;">Extraction</p> <p>Manual compilation in Excel datasheet from original publications</p>

Criteria for inclusion in the newly compiled reference dataset:

- Köppen classification with a buffer of 250 km in the Mediterranean basin
- Availability of:
 - Bulk density
 - Soil organic carbon % (SOC)
 - Texture (Clay, Silt, Sand)
- Land use: agricultural soil (CORINE database*)
- Rock fragments < 5%
- Depth < 1.2 meters

Quality Checking

0.9 < Bulk Density < 2

Predictors based on soil properties

Mean depth, texture, SOC. Computation of power terms and interaction between variables:
Clay², Sand², SOC^{0.5}, SOC², Clay x SOC, Clay x Sand, Clay² x SOC²

Additional data, compiled from WorldClim Bioclimatic data (Annual Mean T°C (BIO1), Mean Diurnal T°C Range (BIO2), Isothermality (BIO3), Temperature Seasonality (BIO4), Max T°C of the Warmest Month (BIO5), Min T°C of the Coldest Month (BIO6), Annual T°C Range (BIO7), Mean T°C of the Wettest Quarter (BIO8), Mean T°C of the Driest Quarter (BIO9), Mean T°C of the Warmest Quarter (BIO10), Mean T°C of the Coldest Quarter (BIO11), Annual Precipitation (BIO12), Precipitation of the Wettest Month (BIO13), Precipitation of the Driest Month (BIO14), Precipitation Seasonality (BIO15), Precipitation of the Wettest Quarter (BIO16), Precipitation of the Driest Quarter (BIO17), Precipitation of the Warmest Quarter (BIO18), Precipitation of the Coldest Quarter (BIO19))

Topographic data (Elevation, Slope, Northness, Profile curvature, Plan curvature)

Extraction per location using GIS

173

174 *Figure 1. Features of the datasets used to train and validate (training and model transferability)*
 175 *three new pedotransfer functions (PTF) for arable soils in the Mediterranean. For a description*
 176 *of the WorldClim Bioclimatic data, please see (Fick and Hijmans, 2017).*

177

178 **2.2 Data used in the training and validation stages**

179

180 *2.2.1. Soil datasets*

181

182 *Training dataset used for PTFs model development:* The World Soil Information Service WoSIS

183 (<https://www.isric.org/explore/wosis>) was used to retrieve soil textural values, SOC content and

184 bulk density. WoSIS is a world scale database containing 196,000 geo-referenced, standardized

185 soil profile entries for soil data from multiple origins. Approximately 40 different organizations

186 around the world provide free access to the data via WoSIS and the Soil Profile

187 (<https://www.isric.org/explore/wosis/wosis-contributing-institutions-and-experts>). More

188 information on WoSIS inclusion criteria, quality assurance, and standardization procedures are

189 available in Batjes et al. (2017). We note that for Europe, one of the main providers of WoSIS data

190 is the Joint Research Center of the European Community, which has made available the entire

191 collection of soil profiles included within the Soil Profile Analytical Database (SPADE-2) (de

192 Souza et al., 2016; Hiederer et al., 2006; Panagos et al., 2013). Using ARCGIS, we selected all the

193 profiles of the WoSIS database belonging to the Mediterranean basin (and defined surrounding

194 areas) with geographic coordinates in metric resolution as well as attributes including sand, silt,

195 clay, organic carbon and bulk density data in at least one soil horizon.

196 *External dataset used to test model transferability:* To assess the model transferability, validation

197 of the three developed PTFs was required. Accordingly, we conducted a systematic literature

198 analysis to collate information on soil textures, SOC, and BD from studies of field crops cultivated

199 on mineral soils in Mediterranean basin and close surrounding areas. The search was carried out

200 in SCOPUS and Web of Science (WoS). The selection criterion was the same as that applied during

201 the extraction of the WoSIS data: required data were BD, SOC, texture and geo-localization. It is

202 needed to remark that systematic queries did not result in a adequate number of suitable articles,
203 so that we used different approaches such as searching for soil dataset within agronomic journals.
204 To compare the performances of the PTF models developed in this study with well-known
205 approaches, in the validation phase we applied the MJ PTF (1991; $BD = 1.660 - 0.318 \cdot SOC^{0.5}$)
206 and we fitted the available SoilGrids BD values (Hengl et al., 2017) with the data of the external
207 validation database constructed as above. SoilGrids is a system for digital soil mapping that uses
208 machine learning methods to map the spatial distribution of soil properties across the globe using
209 WoSIS data and environmental predictors.

210 For both training and validation datasets, the analysis focused on samples that alternatively fall
211 within the 0-0.4 m layer (i.e. topsoil) or the 0.4-1.2 m layer (i.e. subsoil). Due to the presence of
212 multiple horizons inside the topsoil and subsoil, single observations which are part of the training
213 dataset were not averaged. The soil sampling depth were considered as predictor. Furthermore, the
214 inclusion of predictors such as soil properties (soil particle size fractions and SOC stock) allows
215 to describe the soil sample at the given profile depth (e.g., SOC and clay content tend to decrease
216 along the soil profile).

217 The data points used in the training phase which were derived from WoSIS were 129 and 180 for
218 topsoil and subsoil, respectively.

219 As SoilGrids data are provided for six soil layers at the fixed depths (0-5, 5-15, 15-30, 30-60, 60-
220 100, 100-200 cm), we computed a weighted average of SoilGrids BD for the comparison with the
221 BD from the external dataset. For example, if BD is measured for the 10-25 layer then 5 cm belongs
222 to the 5-15 cm SoilGrids layer and 10 cm to the 15-30 cm layer. Consequently, to obtain the sample
223 value, we computed a weighted mean between the SoilGrids BD values given for the 5-15 and the
224 15-30 layers, using a weighting factor of 5 and 10 for the two layers, respectively. We excluded

225 the BD values lower than 0.9 Mg m^{-3} because they were not representative of mineral soils in
226 semiarid regions and, when present, they were likely due to tillage operations occurred close to
227 the sampling moment. We also excluded BD values greater than 2 Mg m^{-3} because they are not
228 representative for agricultural land. Textural plots were prepared using the ggtern software
229 (Hamilton and Ferry, 2018).

230 2.2.2. Geodata

231
232 For the terrain analysis, the Shuttle radar topography mission SRTM 30 m DEM (Farr et al., 2007)
233 was used to obtain topographic data with a resampling at 90 m. The digital elevation model was
234 downloaded in ten tiles from the open topography website (<https://opentopography.org/>). The
235 topographic indices were obtained for the whole study area using the geo-processing terrain
236 analysis tool in SAGA (Conrad et al., 2015). Data pre-processing and maps were prepared using
237 ArcGIS. The WorldClim climatic data (Fick and Hijmans, 2017) was used to obtain climatic data
238 (e.g., mean annual rainfall, average annual temperature). For EU countries, CORINE land cover
239 (Bossard et al., 2000) was used to select agricultural land use. To assign the target land cover
240 (Agriculture) CLC was check for all the available periods, 2000, 2006, 2012, 2018. For non-EU
241 countries – except for Turkey, which was included in CORINE land cover data – we selected soil
242 profiles belonging to agricultural areas by observing satellite and aerial imagery available in
243 ArcMap and Google Earth-Pro.

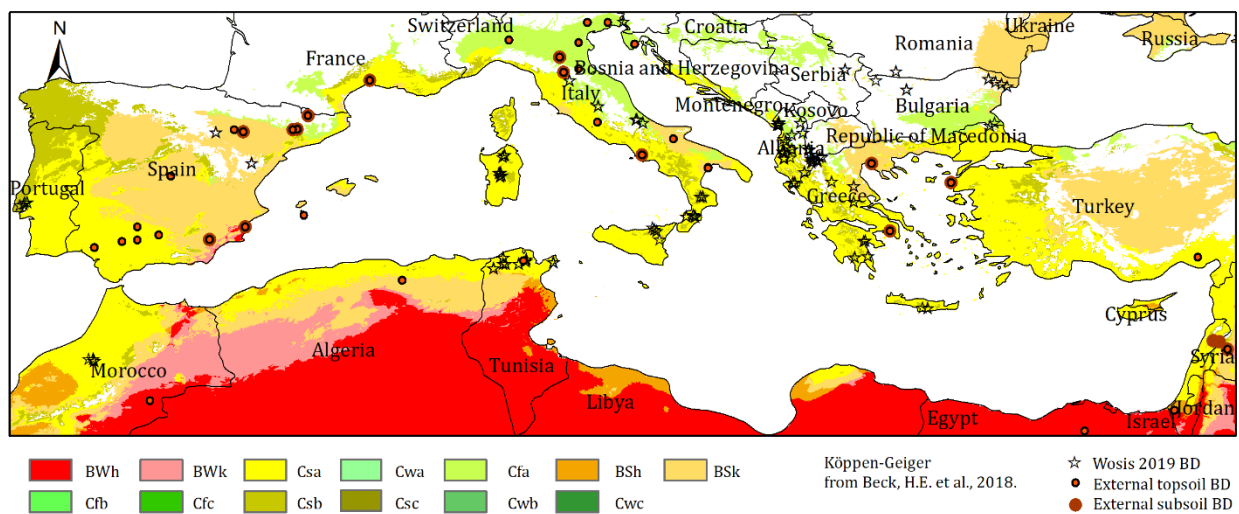
244 2.3. Study area

245 The study focused on the Mediterranean Basin, which covers the territory between 30° and 45°
246 latitudes and, according to the Köppen climate classification system, belongs to the three main
247 climate groups: *B* (dry), *C* (temperate), and *D* (continental) (Francaviglia et al., 2020) (see Fig. 2).
248 The influence of the sea plays a key role in shaping the environment including relief characteristics,

249 which determine the characteristic Mediterranean climate at basin scale (Lionello et al., 2006).
 250 Mediterranean soils are the result of a complex genesis (Lagacherie et al., 2018). Carbonatic and
 251 limestone parent materials are the most widespread minerals in the Mediterranean (Verheye and
 252 De La Rosa, 2005; Zdruli et al., 2011). Long-term agricultural use has altered soil structure and
 253 degraded carbon content. Soil characteristics indicate different ages of soil development and
 254 depths and there is evidence of clay particle translocation within the soil profile (Zdruli et al.,
 255 2011).

256 According to the World Reference Base for Soil Resources (WRB 2006), approximately a dozen
 257 soil orders can be found in the Mediterranean basin: histosols, anthrosols, leptosols, vertisols,
 258 fluvisols, gleysols, andosols, kastanozems and phaeozems, umbrisols, gypsisols, durisols,
 259 calcisols, luvisols, arenosols, cambisols, and regosols. A brief description of these soil orders can
 260 be found in Zdruli et al., (2011). Figure 2 shows the locations of the sites included in the training
 261 (WoSIS data) and validation (extracted from the literature) datasets.

262



263

264 *Figure 2. Study area. The location of the sampling sites (WoSIS data for training and external*
 265 *data for model transferability).*

266 **2.4 Development of PTFs to estimate BD**

267 In this study, we evaluated three methods to estimate BD, namely Multiple Linear Regression
268 (MLR) models each using two-variable selection criteria, and Artificial Neural Networks (ANN).
269 These methods were chosen in our analyses because they are suitable when data are sparse and no
270 spatial structure can be defined. A 10-fold cross-validation frame was used to assess the prediction
271 accuracy (Veronesi and Schillaci, 2019). The three models were defined using a wide set of
272 predictors, i.e. independent variables (soil properties, bioclimatic and topographic indicators).
273 These predictors were derived from the soil and additional database (Fig. 1).

274

275 *2.4.1 Multiple linear regression (MLR)*

276

277 The first method (MLR-S) used was a stepwise multiple linear regression starting from no
278 dependent variables (a constant-only model); the first dependent variable that will be included in
279 the model is the variable that produces the maximum increase in R^2 ; if the increase in the
280 explicated variance is significant (partial F test) at a given $P(F)$, called inclusion threshold, the
281 variable is retained in the model (forward step). The same procedure is done to evaluate the
282 possibility to include a second independent variable and so on. At each inclusion step, there is an
283 exclusion step too, where, among the variables included in the model, the variable that is excluded
284 causes the lower reduction in explicated variance. If the decrease of explained variability is not
285 significant at a given $P(F)$, called exclusion threshold and higher than the inclusion threshold, the
286 variable is excluded from the model. The process stops when no more dependent variables are
287 included or excluded (Noryani et al., 2019).. In the MLR-S, a predictor is included in the model if
288 its regression coefficient is significant at $P \leq 0.05$ and excluded if the partial F test has a $P > 0.1$
289 (Draper and Smith, 1998).

290 The second approach was a stepwise variable selection, which started by including all independent
291 variables, then excluded non-significant variables one by one using a backward stepwise approach
292 (MLR-BS). Variables were excluded when their contribution did not affect the model explication
293 capability (i.e., when the partial F test have a $P > 0.1$) (Ghani and Ahmad, 2010).

294 For both methods (MLR-S and MLR-BS), the normality test of Kolmogorov-Smirnov and the
295 Breush-Pagan test for the homogeneity of variances (Breusch et al., 1979) were applied to the
296 residuals of the regression models.

297 *2.4.2 Artificial Neural Network*

298
299 An ANN is part of a computing system, which is developed to mimic the way the human brain
300 processes information. ANN allows finding non-linear behavior of the system that cannot be
301 discovered with traditional regression-based methods. To develop a PTF, the ANN is generally
302 made by three layers of neurons, i.e. an input layer, a hidden layer and an output layer (Ebrahimi
303 et al., 2019; Minasny and McBratney, 2002; Schaap et al., 1998). This kind of ANN architecture
304 is known as Multi-Layer Perceptron (MLP). ANN imposes minimal requirements for model
305 structure or assumptions because the shape of the relationship is determined during the learning
306 process (Haykin, 2008). We used an MLP implementation in the IBM-SPSS 26.0.0.1. One hidden
307 layer was used with three neurons according to the default settings, using the hyperbolic tangent
308 activation function and the identity function for the output layer. This is an identity function
309 because this task is a regression problem. The weighted connections feed forward from the input
310 layer to the output layer. The training algorithm works by back-propagating the prediction error,
311 through the parameters of the neural network. In this study, the MLP had 18 input predictors and
312 one output variable, i.e. BD. The independent variables used as predictors in the three statistical
313 models for the BD estimation are shown in Fig. 1. The optimal fit was reached in cross-validation

314 by using 1 hidden layer, combined with three neurons. The Hyperparameters tuning was iteratively
315 tested by applying an ANN with one hidden layer with 2 to 10 neurons and, alternatively, an ANN
316 with two hidden layers with 2 to 5 neurons in the first hidden layer combined with 2 or 3 neurons
317 in the second hidden layer. The use of one single hidden layer resulted to be more effective. This
318 result agreed with the automatic parameterization proposed by the software:
319 ([ftp://public.dhe.ibm.com/software/analytics/spss/documentation/statistics/27.0/en/client/Manual](ftp://public.dhe.ibm.com/software/analytics/spss/documentation/statistics/27.0/en/client/Manuals/IBM_SPSS_Statistics_Algorithms.pdf)
320 [s/IBM_SPSS_Statistics_Algorithms.pdf](ftp://public.dhe.ibm.com/software/analytics/spss/documentation/statistics/27.0/en/client/Manuals/IBM_SPSS_Statistics_Algorithms.pdf)). Regarding computation time, the model training phase
321 takes few second.

322 2.5. Analysis of models' performance

323
324 The following evaluation indices were calculated to test the model performance in estimating BD:

- 325 i) R^2 coefficient of determination of the scatter plot of the predicted against the observed values;
326 ii) Bias and %Bias (Addiscott and Whitmore, 1987), optimal value is 0, range is from $+\infty$ to $-\infty$;
327 when the Bias% is $< 10\%$ it may be considered very favorable (Moriassi et al., 2007);
328 iii) Root Mean Square Error (RMSE) and %RMSE ($RMSE / (\text{Observed Mean}) * 100$) (Fox, 1981),
329 optimal value is 0, range is from 0 to $+\infty$; %RMSE value lower than 10% is considered to be
330 favorable (Bellocchi et al., 2002);
331 iv) The Pearson correlation coefficient, optimal value is 1, range is from +1 to -1;
332 v) The slope of the regression of observed data to the estimated ones, optimal value is 1, range is
333 from $+\infty$ to $-\infty$ (Piñeiro et al., 2008).

334 Note that Bias is always equal to 0 when the ordinary least square (OLS) method is applied, which
335 was the case in the two regression training sets. Moreover, in OLS analysis the slope of observed
336 values against the estimated values is equal to 1. All indices were computed using Irene-DLL (Fila
337 et al., 2003).

338 3. Results

339 3.1 Descriptive statistics

340 3.1.1 *Soil properties*

341
342 The highest average BD value was observed in the subsoil training dataset ($1.51 \pm 0.17 \text{ Mg m}^{-3}$).

343 The lowest average BD value was observed in the topsoil validation dataset ($1.38 \pm 0.12 \text{ Mg m}^{-3}$).

344 The SOC was higher in the topsoil testing ($1.28 \pm 1 \%$), and lower in the subsoil testing dataset
345 ($0.61 \pm 0.35 \%$) (Table 3). The most variable soil property was the sand content with a coefficient

346 of variation ranging from 48 to 85%, while BD was less variable with a coefficient of variation

347 ranging from 9 to 14%. The references of the independent dataset for validation are listed in Table

348 2. The independent external dataset for validation comprised 59 observations for the topsoil and

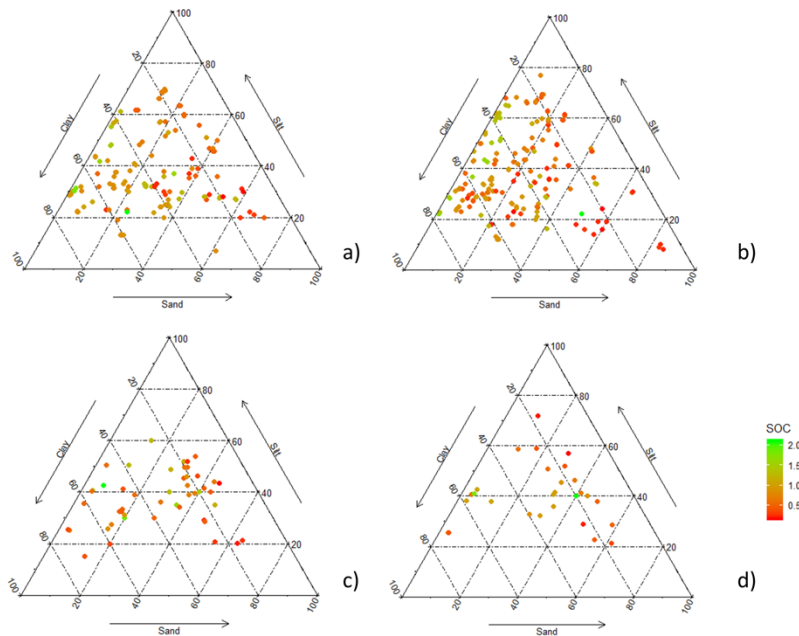
349 29 for the subsoil, Table 3. Textural plots of the training and validation datasets are shown in Table

350 3.

351

Table 2. Independent dataset for validation with country, climate and reference.

Country	Köppen climate classification	Author
Algeria	BSk	Chennafi et al., 2006
Croatia	Cfa	Bogunovic et al., 2018
Egypt	BWh	Mahmoud et al., 2019
	BWh	Salem et al., 2015
	BWh	Zohry et al., 2017
France	Csa	Cardinael et al., 2017
Greece	CSa	Antonopoulos et al., 2013
Israel	BSh	Stavi et al., 2008
Italy	Cfa	Pezzuolo et al., 2017
	Cfa	Carozzi et al., 2013
	Csa	Francaviglia et al., 2015
	Cfa	Valboa et al., 2015
	Cfa	Perego et al., 2019
	Cfa	Ceotto et al., 2018
	Cfa	Diacono et al., 2018
	Csa	Vitale et al., 2017
	Csa	Karam et al., 2007
Lebanon	Csa	Ichir et al., 2003
Morocco	Csa	Ichir et al., 2003
	BSk	Pareja-Sánchez et al., 2017
	Cfa	Bescansa et al., 2006
	BSk	Pardo et al., 2020
	BSk	Tolon-Becerra et al., 2011
	Bsk-Cfa	Álvaro-Fuentes et al., 2008
	BWh	Visconti et al., 2019
	BSk	Recio et al., 2018
	Csa	Marquez-Garcia et al., 2013
	Csa	Marquez-Garcia et al., 2013
Syria	Bsk	Abou Zakhem et al., 2019
Tunisia	Csa	Jemai et al., 2013
Turkey	Csb	Çelik et al., 2019



354

355 *Figure 3. Textural plots, a) topsoil validation dataset, b) subsoil validation dataset, c) topsoil test*
 356 *dataset d) subsoil test dataset.*

357

358

359 **Table 3. Soil properties of the training and testing data for topsoil (0-0.4m) and subsoil (0.4-1.2**
 360 **m): Bulk Density (BD), Soil Organic Carbon (SOC), Fine earth fractions,**

		BD (Mg m⁻³)	SOC (%)	Sand (%)	Silt (%)	Clay (%)
Topsoil Training	mean	1.44	1.26	24.4	36.5	39.1
(N=129)	Stdv	0.20	0.64	17.1	14.1	18.1
Topsoil Testing	mean	1.41	1.28	31.39	40.68	28.21
(N=59)	Stdv	0.11	1.0	13.82	9.09	14.25
Subsoil Training	mean	1.51	1.15	20.1	38.2	41.7
(N=180)	Stdv	0.17	0.67	17.0	15.7	17.4
Subsoil Testing	mean	1.48	0.61	29.04	39.49	31.56
(N=29)	Stdv	0.16	0.35	19.38	12.58	18.4

361

362

363 *3.1.2 Environmental variables*

364

365 Average precipitation reported in the training dataset was highly variable in the study area with a

366 minimum value of 426 and a maximum of 1693 mm yr⁻¹. The validation dataset showed a

367 minimum annual rainfall of 189 and a maximum of 1155 mm yr⁻¹. Mean annual temperature,
 368 Elevation (m), Slope (%) are reported in Table 4.

369 *Table 4. Descriptive statistics of the selected environmental variables*

		Annual Average Precipitation (mm yr ⁻¹)	Mean annual temperature (° C)	Elevation (m)	Slope (%)
Training (N=77 sites)	mean	774.4	10.5	321	4.3
	stdv	294.4	1.5	332	5.4
Testing (N=36 sites)	mean	495.7	16	318	4
	stdv	300	3.1	379	4.9

370

371 **3.2 Model performance and transferability**

372 Homogeneity of variance and normality tests for the MLR models were conducted using the
 373 Breush-Pagan test and Kolmogorov-Smirnov test (Table 5).

374 *Table. 5 Homogeneity of variance and normality tests for Multiple Linear Regression (MLR)*
 375 *models.*

	MLR-S		MLR-BS	
	Topsoil	Subsoil	Topsoil	Subsoil
Homogeneity of variance of residuals*	0.056	0.051	0.065	0.051
Normality of residuals**	>0.2	>0.2	>0.2	>0.2

376 *Breush-Pagan test; ** Kolmogorow-Smirnov test

377 Topsoil model metrics are shown in Table 6. The RMSE of the topsoil training dataset (Table 6a)
 378 ranged from 0.07 (ANN) to 0.17 (MLR-S), and similar performances were obtained with the MLR-
 379 BS models. The Bias of the ANN was close to zero. The ANN model showed the highest R² (0.89),
 380 whereas the MLR-S model showed the lowest R² (0.24).

381 *Table 6. Performance of the newly developed pedotransfer function (PTF) as developed with the*
 382 *topsoil training and cross validation (a) and tested with the independent external datasets for*
 383 *model transferability (b). Indices values reported in brackets refer to the cross-validation results.*

	MLR-S	- MLR-BS	- ANN	- ANN	
a)	MLR-S CV	MLR-BS CV	CV		
RMSE	0.17 (0.16)	0.14 (0.15)	0.07 (0.16)		
rRMSE %	11.91 (11.53)	9.68 (10.81)	4.56 (11.4)		
Bias	(0.0007)	(0.0047)	0.00 (0.01)		
Bias %	(0.144)	(0.37)	0.10 (1.11)		
r	0.51 (0.49)	0.72 (0.57)	0.94 (0.67)		
R ²	0.26 (0.33)	0.51 (0.37)	0.89 (0.48)		
Slope b	(0.84)	(0.71)	1.00 (0.78)		
Estimated Max	1.61 (1.6)	1.80 (1.67)	1.90 7 (1.75)		
Estimated Min	1.16 (1.22)	1.02 (1.14)	0.88 (1.13)		
N	129				
b)	MLR-S	MLR-BS	ANN	MJ	SoilGrids
RMSE	0.14	0.32	0.16	0.17	0.13
rRMSE %	9.28	22.26	11.53	11.93	9.12
Bias	0.06	0.13	0.07	-0.11	0.008
Bias %	1.1	11.2	1.4	-6.657	0.04
r	0.34	0.05	0.64	0.24	0.09
R ²	0.12	0.00	0.41	0.06	0.01
Slope b	0.29	-0.12	1.11	0.23	0.05
Estimated Max	1.7	2.75	1.94	1.44	1.53
Estimated Min	1.24	1.03	0.92	0.76	1.28
N	59				

384

385 The RMSE in the topsoil validation dataset (Table 6b) range from 0.13 (SoilGrids) to 0.32 (MLR-
386 BS). All the Bias values were ≤ 0.5 . The R² ranged between 0.09 to 0.41, in SoilGrids and ANN,
387 respectively.

388

389

390

391 *Table 7. Performance of the newly developed pedotransfer function (PTF) as developed with the*
392 *subsoil training and cross validation (a) and tested with the independent external datasets for*
393 *model transferability (b). Indices values reported in brackets refer to the cross-validation results.*

394

a)	MLR-S	MLR-BS	ANN
RMSE	0.14 (0.13)	0.12 (0.13)	0.07 (0.11)
rRMSE %	9.04 (9.24)	8.04 (8.67)	4.53 (7.79)
Bias	(-0.0003)	(-0.0004)	0.00 (0.003)
Bias %	(0.0056)	(0.0008)	-0.16 (0.21)
r	0.49 (0.47)	0.70 (0.58)	0.92 (0.67)
R ²	0.24 (0.21)	0.48 (0.38)	0.84 (0.48)
Slope b	(0.90)	(0.90)	0.98 (0.84)
Estimated Max	1.77 (1.68)	1.79 (1.71)	1.93 (1.76)
Estimated Min	1.12 (1.32)	1.35 (1.28)	1.10 (1.26)
N	180	180	180

b)	MLR-S	MLR-BS	ANN	MJ	SoilGrids
RMSE	0.17	0.39	0.21	0.14	0.17
rRMSE %	11.78	26.26	13.93	9.54	11.39
Bias	0.09	-0.04	0.15	-0.07	0.07
Bias %	2.8	-2.347	1.7	-4.66	0.708
r	0.38	0.35	0.67	0.26	-0.42
R ²	0.15	0.13	0.45	0.07	0.18
Slope b	0.37	1.06	0.94	0.001	-0.11
Estimated Max	1.99	1.95	1.88	1.53	1.64
Estimated Min	1.38	1.01	1.29	1.20	1.47
N	30				

395

396 Subsoil model metrics are shown in Table 7. The RMSE in the subsoil training dataset (Table 7a)

397 ranged from 0.07 (ANN) to 0.14 (MLR-S). The Bias of the ANN was close to zero. The ANN

398 model showed the highest R² of 0.84, whereas the MLR-S model showed the lowest R² of 0.24.

399 The RMSE in the subsoil external dataset (Table 7b) are very similar and ranged from 0.14 to 0.39.

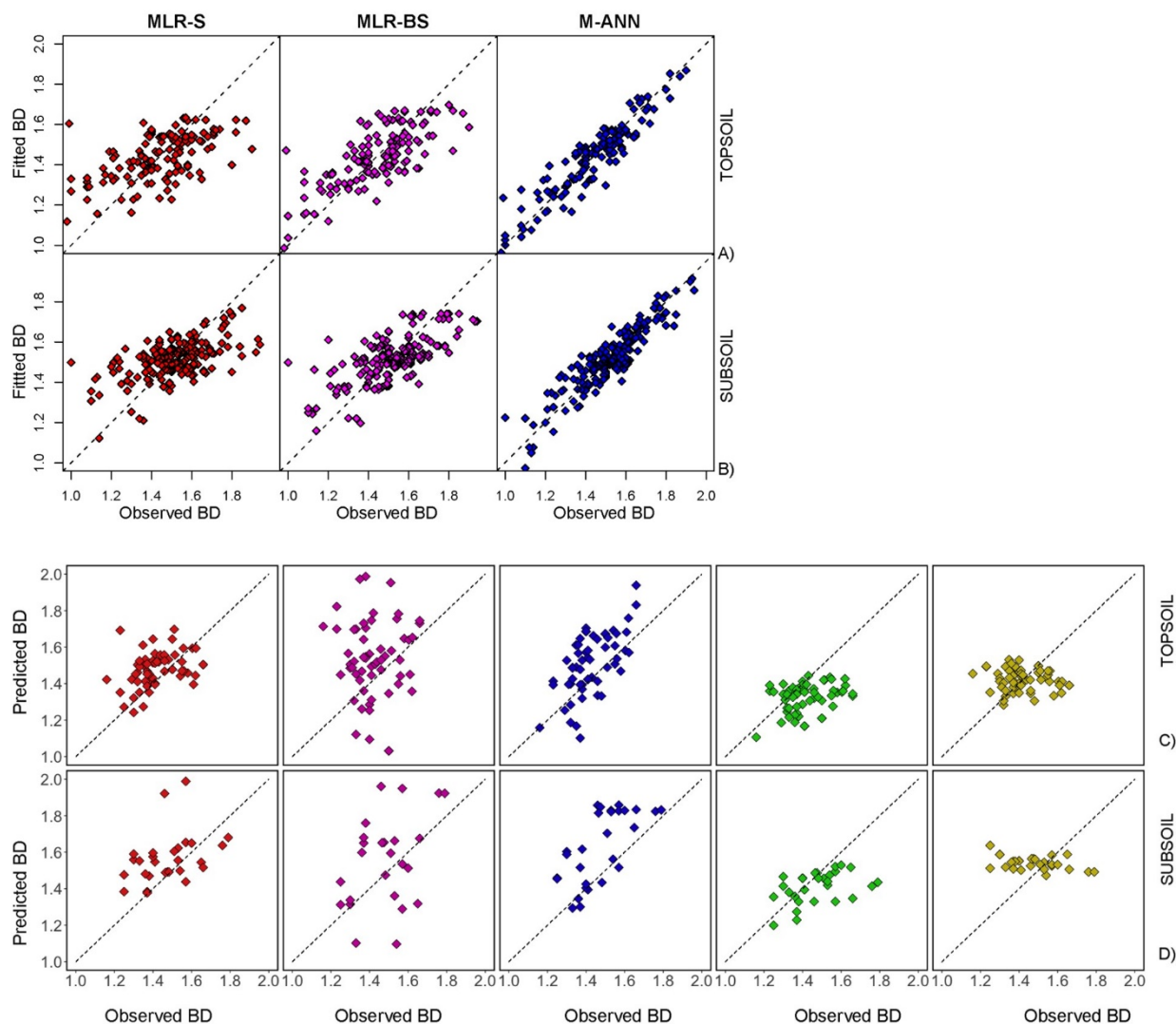
400 The Bias % values ranging from -4.6 (MJ) to 2.8% (MLR-S). The R² ranged between 0.07 (MLR-

401 S) to 0.45 (ANN), respectively.

402 Since the best performance was achieved with the ANN, we provide a .xlm spreadsheet file that

403 can be used to execute the PTF developed with the ANN using the soil data, topography and

404 WorldClim. Furthermore, to allow users to apply the PTF based on the ANN in different statistical
 405 packages a Predictive Model Markup Language file (PMML), which is an XML-based predictive
 406 model interchange format, is available in the supplemental materials.



407
 408 *Figure 4. Predicted vs observed data (training topsoil and subsoil A and B, validation topsoil and*
 409 *subsoil C and D), MLR-S model, MLR-BS model, ANN neural network model, MJ PTF SoilGrids.*
 410 **3.3 Variable importance**

411 Table 8 shows the absolute standardized regression coefficient for each MLR model, considering
 412 100% the highest beta value, to obtain a comparable result to the ANN model. Clay was the most
 413 important predictor in the topsoil MLR-S model. In the topsoil, SOC contributed approximately

414 25% of BD in the MLR-BS PTF, but it was not present in the MLR-S models. Similarly, Clay²
 415 was not present in the MLR-S models, slope and SOC² were the most important predictors in the
 416 subsoil using MLR-BS. Bioclimatic predictors such as BIO1 (Annual Mean Temperature), BIO2
 417 (Mean Diurnal) and BIO7 (Annual T°C Range) were the most influential predictors in both topsoil
 418 and subsoil using MLR models. In topsoils, predictors included BIO7 (Annual T°C Range) and
 419 BIO14 (Precipitation of the Driest Month), heavily contributed to BD estimates within the MLR-
 420 BS and MLR-S of BD. BIO7 (Annual T°C Range) was more important than BIO14 (Precipitation
 421 of the Driest Month) in any model. Among the topographic predictors, the elevation was important
 422 in subsoil MLR-S models (contributing 24%), whereas it was not important in the topsoil or subsoil
 423 MLR-BS models. In subsoils, BIO3 (Isothermality) contributed 8% and 7% of subsoil BD in
 424 MLR-S and MLR-BS.

425 *Table 8 Normalized variable importance in the MLR-S and MLR-BS (standardized regression*
 426 *coefficient in %). Conditional formatting is applied, Red color marks the minimum, green color*
 427 *the maximum and the yellow marks the middle values.*
 428

	MLR-S TOP	MLR-BS TOP	MLR-S SUB	MLR-BS SUB
Clay				4.62
Sand		5.83		
Silt		2.97	14.67	
SOC		19.15		4.69
MeanDepth			11.73	
Elevation		2.34		4.53
Slope			24.97	4.35
Profile Curvature			13.91	
BIO1				5.70
BIO2		11.23		5.91
BIO3		8.73		6.01
BIO4	36.46			
BIO5		4.59		5.20
BIO7	46.88	7.56	14.75	4.90
BIO12				6.09
BIO13				5.26
BIO14	16.67	1.21		5.02
BIO15		1.90		
BIO17				5.08
BIO18				4.85

BIO19			4.74
Clay ²	3.17		4.57
Sand ²	2.14		
SOC ²	6.10	19.96	4.81
SOC ² *Clay ²	3.98		4.76
SOC ^{0.5}	14.22		4.15
Clay*SOC	4.87		4.78

429

430 Table 9 shows the importance of the predictors included in the ANN models, based on sensitivity
431 analyses using the default option in the MLP tool in IBM SPSS (independent variable importance
432 analysis). The models included all the predictors except interactions between soil properties which
433 were calculated within the ANN procedure but hidden to the user. Among the main physical and
434 chemical properties, Sand was the most important in topsoil (5.6) and SOC in subsoil (5.5)
435 Within the ANN, the most important predictors were BIO7 (Annual T°C Range) and Profile
436 Curvature for topsoil and subsoil, respectively. Other important predictors were MeanDepth and
437 the BIO12 (Annual Rainfall) in topsoil. SOC, BIO1 (Annual Mean Temperature) and BIO16
438 (Precipitation of the Wettest Quarter) were important in topsoil and subsoil. Soil properties
439 predicted the BD of subsoil. Clay predicted BD in subsoil (3.2) and topsoil (2.8). Among the
440 topographic predictors, Profile and plan curvature played a stronger role predicting the BD of the
441 topsoil (5.3) compared to the subsoil (5.6).

442

443 *Table 9. Normalized variable* importance for predicting the bulk density of the top- and subsoil*
444 *by means of the pedotransfer function developed by the Artificial Neural Network optimization*
445 *approach. *variable description is available in figure 1, Conditional formatting is applied, Red*
446 *color marks the minimum, green color the maximum and the yellow marks the middle values.*

447

	Topsoil	Subsoil
Clay	3.2	2.8
Sand	5.6	1.2
Silt	3.4	3.7
SOC	3.8	5.5
MeanDepth	1.4	1.5

Elevation	3.8	2.7
Slope	2.6	5.3
SIN Aspect	3.3	1.7
Profile Curvature	5.3	4.5
Plan Curvature	3.8	5.6
BIO1	2.5	2.8
BIO2	5.3	5.0
BIO3	2.0	2.7
BIO4	3.7	4.4
BIO5	4.7	1.6
BIO6	3.4	1.8
BIO7	3.9	5.4
BIO8	3.5	4.0
BIO9	3.8	2.9
BIO10	1.6	2.6
BIO11	2.9	1.8
BIO12	1.4	2.6
BIO13	3.0	2.3
BIO14	3.2	3.2
BIO15	5.6	2.3
BIO16	3.3	1.8
BIO17	3.9	3.5
BIO18	4.4	3.3
BIO19	1.7	2.7

448

449 **4 Discussion**

450 Collaborative work among researchers from different branches of geosciences facilitated a
 451 systematic literature review and compilation of an up-to-date, regionally-relevant geo-dataset; and
 452 this permitted the development and validation of new pedotransfer functions (PTF) to predict the
 453 BD of top- and subsoil in the Mediterranean.

454

455 **4.1 Performance of pedotransfer functions**

456 In this study, the performances of three new PTFs to estimate BD (MLR-S, MLR-BS and ANN)
 457 were defined used WoSIS soil data in combination with environmental data. The model

458 transferability of the new PTFs was carried out using external dataset from Mediterranean
459 locations derived from literature. Results were also benchmarked against the widely used MJ-PTF,
460 which uses only soil organic carbon to predict BD, and the global SoilGrids data which are based
461 on topographic and remote-sensed estimates of BD. Among the MLR approaches, MLR-BS
462 performed slightly better than MLR-S. The ANN model outperformed the MLR models.

463 Our PTF development strategy, which implies the use of topographic and climatic variables along
464 with soil properties, agreed with the approach of Wang et al., (2014) and Akpa et al., (2016).
465 However, we also validated our new PTFs by estimating the BD in top- and subsoil using an
466 external and independent dataset. This resulted in less accurate predictions than those made by the
467 training datasets as already remarked by (Khaledian and Miller, 2020; Morin and Davis, 2017;
468 Thompson, 2006). Nevertheless, these authors suggested that the use of external dataset rather than
469 internal validation methods provides direct evidence about whether study results will replicate
470 (Thompson, 2006).

471 Here we initially used MLR because it is a hands-on tool that provides direct quantitative and
472 easily interpretable results. By contrast, the ANN has provided an alternative machine learning
473 approach used in relatively recent analyses (Alvarez-Acosta et al., 2012; Ballabio et al., 2016;
474 Chen et al., 2018; Ghehi et al., 2012; Nussbaum et al., 2018). In this study, the MJ PTF was used
475 as a simple comparator because it is independent of other physical soil parameters except SOC and
476 is the most widely used PTF. In our MLR-BS topsoil, MLR-S subsoil, and MLR-BS subsoil
477 models, we considered inclusion of the key determinant used (i.e., SOC square root), but it was
478 not included in the final model because it did not significantly improve the predictions. Our MLR-
479 S and MLR-BS performed better than the MJ because our dataset included additional factors that
480 directly determine BD over the long-term (such as those related to the climate or topography), thus

481 raising the prediction capability. the SoilGrids database yielded a lower prediction ability in
482 comparison to the other models. SoilGrids is considered as an interesting solution because it is a
483 gridded multiple depth dataset at a 250m spatial resolution and it is available worldwide. However,
484 the present results suggest that SoilGrids BD estimations may not adequately match the observed
485 BD values (i.e., external dataset) which were measured in specific sites located in the
486 Mediterranean area.

487 **4.2 Data groupings and reliability of PTFs**

488 The fit of the MLR subsoil models was more satisfactory than for subsoil linear model MLR-S
489 with an R^2 0.12. Subsoil models were also more satisfactory for the ANN ($R^2 = 0.45$). This is in
490 contrast to previous publications in which grouping input data by soil depths did not improve the
491 prediction of BD in tropical soils (De Vos et al., 2005), which might have been attributable to
492 different level of disturbance of the soil in the study areas (Hollis et al., 2012), or differences in
493 the additional factors analyzed.

494 Arable soils undergo significant changes over time due to tillage and cultivation. Therefore,
495 physical soil properties such as BD are more stable in the subsoil than in the topsoil. Statistics for
496 soil texture and SOC agreed with data reported for other Mediterranean countries (Çelik et al.,
497 2019; Evrendilek et al., 2004). The MJ and SoilGrids models yielded a similar result (Table 6 and
498 7). Notably, MLR-BS showed an R^2 close to zero for the validation datasets. This hampers
499 discussion of model variability comparing the training and validation datasets. Generally, negative
500 Bias is observed in the subsoil external dataset. As for the external dataset, slightly positive Bias
501 indicates that MLR-S, ANN, SoilGrids overestimate the average BD of 2.8%, 1.7 % and 0.7%,
502 respectively; MJ and MLR-BS underestimate the BD of -4.6% and -2.3% which is not preferable
503 especially for the subsoil, an exception has been encountered with the topsoil MLR-BS that has

504 predicted in few cases values very far from the true BD. Mediterranean soils are diverse, their
505 hydraulic properties reflect pedogenetic factors as well as recent changes in management and
506 climate (Yaalon, 1997).

507 **4.3 Importance of predictor variables**

508 Previous attempts to estimate soil BD by PTF (Çelik et al., 2019; Gozubuyuk et al., 2014; Tranter
509 et al., 2007) did not include climate parameters because they were often not readily available or
510 not immediately obvious as a determinant of BD. Many factors related to climate, such as
511 bioclimatic indices, affect BD (e.g., rainfall intensity or pattern, high soil temperature in summer)
512 (Basile et al., 2019; Chen et al., 2018). Bioclimatic indices and topographic predictors contributed
513 greatly to the performance of the MLR and comprised 100% of the variables in the MLR-S for the
514 topsoil, and about the 33% in the MLR-BS. The regression models (MLR-S and MLR-BS)
515 included soil textural data (MLR-S topsoil) or SOC related (MLR-S subsoil and MLR-BS topsoil
516 and subsoil). Our results showed that important predictors of BD in the MLR models were slope,
517 clay, SOC², and bioclimatic variables such as BIO1 (Annual Mean Temperature), BIO2 (Mean
518 Diurnal Range) and BIO7 (Annual T°C Range). This is consistent with previous reports (Akpa et
519 al., 2016). In fact, part of the BD variability is due to the diverse bioclimatic zones within the
520 Mediterranean Basin (Beck et al., 2018).

521 In our study, the inclusion of the climatic and topographic data increased the model reliability.
522 Indeed, models without topographic and climatic predictors had very low performance at the
523 training stage (data not shown). However, the lack of field management information, which
524 strongly affects arable soils (e.g., crop type, tillage methods, irrigation, input of organic matter),
525 hampers the ability to infer a relationship with factors of soil formation and processes (Wadoux
526 et al., 2019) which would potentially improve the model prediction. In the Mediterranean Basin,

527 significant effects of cropping systems and field managements on BD have been demonstrated in
528 field studies (Álvaro-Fuentes et al., 2008; Bogunovic et al., 2020; Çelik et al., 2019; Perego et al.,
529 2019; Pezzuolo et al., 2017).

530 **5. Conclusions**

531 Arable soils are widely distributed and the estimation of their fertility and carbon sequestration
532 ability is a prerequisite for their management at wide scale. Reliable PTF to estimate BD are thus
533 a needed instrument for arable soils management at the regional or higher levels. In the present
534 study, we developed a robust PTF for BD estimation by exploiting the WoSIS resource, and it was
535 the first time that such a broad set of data are valorized for PTF development. Moreover, we
536 considered relevant predictors such as climatic and topographic parameters, which are fully and
537 freely available and responsible for remarkably improving the predictive capability of the PTF
538 models.

539 One of the three developed PTF (i.e., ANN) showed a better capability of estimating BD data than
540 the well-known function Manrique Jones and the SoilGrids estimation approach; this outcome
541 proved that the work hypothesis was correct and then developing the PTF with climate-specific
542 set of data and adding topographic and climate predictors leads to a better predictive capability.

543 A relevant result of the present work is a ready to be used PTF model (i.e., ANN) for to separate
544 soil layers (i.e., topsoil and subsoil) for the arable soils in the Mediterranean basin. The potential
545 users of this result are public authorities interested in estimating soil carbon stock by exploiting
546 legacy soil data in which bulk density is an often-missing parameter in the large monitoring
547 campaigns. Researchers can be also interested in a more robust method of BD estimation when
548 elaborating sets of soil data, especially when the aim is to estimate spatial and temporal variation.

549 The robustness of the ANN PTF is ensured by the use of an independent external dataset compiled
550 from the literature for the validation of the PTF models transferability.
551 Results from the present work provide a reproducible and externally tested tool that can be applied
552 to obtain a BD estimation at a regional level more reliable than the presently used PTF or gridded
553 benchmarks. Thus, the present results are an option for policy making and management at a
554 regional level.

555

556 **6. Acknowledgments**

557 All authors acknowledge the funding for the Lake Como Advanced School provided by the grant
558 for the SDAE Summer School 2019 from the Italian Society of Agronomy, University of Milan
559 and University of Pavia. WLC. Landsupport H2020, grant number ID: 774234. Project “Carbon
560 Market - Innovative cropping systems for carbon market” funded by Natural Resources Institute
561 Finland (Luke). We express our gratitude to Cami Moss for editing the manuscript.

562 Views, thoughts, and opinions expressed in the text belong solely to the author and do not reflect
563 the opinion of the author's employer, organization, committee members, or that of other course
564 participants.

565 This paper is dedicated to the dear memory of Prof: Dario Sacco, who was a teacher of the SDAE
566 School.

567 **References**

568 Acutis, M., Donatelli, M., 2003. SOILPAR 2.00: Software to estimate soil hydrological
569 parameters and functions, in: *European Journal of Agronomy*. pp. 373–377.

570 [https://doi.org/10.1016/S1161-0301\(02\)00128-4](https://doi.org/10.1016/S1161-0301(02)00128-4)

571 Addiscott, T.M., Whitmore, A.P., 1987. Computer simulation of changes in soil mineral nitrogen

572 and crop nitrogen during autumn, winter and spring. *J. Agr. Sci.* 109, 141–157.

573 Aitkenhead, M., Coull, M., 2020. Mapping soil profile depth, bulk density and carbon stock in
574 Scotland using remote sensing and spatial covariates. *Eur. J. Soil Sci.*
575 <https://doi.org/10.1111/ejss.12916>

576 Akpa, S.I.C., Ugbaje, S.U., Bishop, T.F.A., Odeh, I.O.A., 2016. Enhancing pedotransfer
577 functions with environmental data for estimating bulk density and effective cation exchange
578 capacity in a data-sparse situation. *Soil Use Manag.* 32, 644–658.
579 <https://doi.org/10.1111/sum.12310>

580 Alvarez-Acosta, C., Lascano, R.J., Stroosnijder, L., 2012. Test of the Rosetta Pedotransfer
581 Function for Saturated Hydraulic Conductivity. *Open J. Soil Sci.* 02, 203–212.
582 <https://doi.org/10.4236/ojss.2012.23025>

583 Álvaro-Fuentes, J., López, M. V., Cantero-Martinez, C., Arrúe, J.L., 2008. Tillage Effects on
584 Soil Organic Carbon Fractions in Mediterranean Dryland Agroecosystems. *Soil Sci. Soc.*
585 *Am. J.* 72, 541–547. <https://doi.org/10.2136/sssaj2007.0164>

586 Álvaro-Fuentes, J., Paustian, K., 2011. Potential soil carbon sequestration in a semiarid
587 Mediterranean agroecosystem under climate change: Quantifying management and climate
588 effects. *Plant Soil* 338, 261–272. <https://doi.org/10.1007/s11104-010-0304-7>

589 Ballabio, C., Panagos, P., Monatanarella, L., 2016. Mapping topsoil physical properties at
590 European scale using the LUCAS database. *Geoderma* 261, 110–123.
591 <https://doi.org/10.1016/j.geoderma.2015.07.006>

592 Basile, A., Bonfante, A., Coppola, A., De Mascellis, R., Falanga Bolognesi, S., Terribile, F.,
593 Manna, P., 2019. How does PTF Interpret Soil Heterogeneity? A Stochastic Approach
594 Applied to a Case Study on Maize in Northern Italy. *Water* 11, 275.

595 <https://doi.org/10.3390/w11020275>

596 Batjes, N.H., Dijkshoorn, J.A., 1999. Carbon and nitrogen stocks in the soils of the Amazon
597 Region. *Geoderma* 89, 273–286. [https://doi.org/10.1016/S0016-7061\(98\)00086-X](https://doi.org/10.1016/S0016-7061(98)00086-X)

598 Batjes, N.H., Ribeiro, E., van Oostrum, A., Leenaars, J., Hengl, T., Mendes de Jesus, J., 2017.
599 WoSIS: providing standardised soil profile data for the world. *Earth Syst. Sci. Data* 9, 1–14.
600 <https://doi.org/10.5194/essd-9-1-2017>

601 Beck, H.E., Zimmermann, N.E., McVicar, T.R., Vergopolan, N., Berg, A., Wood, E.F., 2018.
602 Present and future köppen-geiger climate classification maps at 1-km resolution. *Sci. Data*
603 5, 1–12. <https://doi.org/10.1038/sdata.2018.214>

604 Bellocchi, G., Acutis, M., Fila, G., Donatelli, M., 2002. An indicator of solar radiation model
605 performance based on a fuzzy expert system. *Agron. J.* 94, 1222–1233.
606 <https://doi.org/10.2134/agronj2002.1222>

607 Benites, V.M., Machado, P.L.O.A., Fidalgo, E.C.C., Coelho, M.R., Madari, B.E., 2007.
608 Pedotransfer functions for estimating soil bulk density from existing soil survey reports in
609 Brazil. *Geoderma* 139, 90–97. <https://doi.org/10.1016/j.geoderma.2007.01.005>

610 Bogunovic, I., Pereira, P., Galic, M., Bilandzija, D., Kistic, I., 2020. Tillage system and farmyard
611 manure impact on soil physical properties, CO₂ emissions, and crop yield in an organic
612 farm located in a Mediterranean environment (Croatia). *Environ. Earth Sci.* 79, 1–11.
613 <https://doi.org/10.1007/s12665-020-8813-z>

614 Bondi, G., Creamer, R., Ferrari, A., Fenton, O., Wall, D., 2018. Using machine learning to
615 predict soil bulk density on the basis of visual parameters: Tools for in-field and post-field
616 evaluation. *Geoderma* 318, 137–147. <https://doi.org/10.1016/j.geoderma.2017.11.035>

617 Bossard, M., Feranec, J., Otahel, J., Steenmans, C., 2000. CORINE land cover technical guide-

618 Addendum 2000.

619 Bouma, J., 1989. Using Soil Survey Data for Quantitative Land Evaluation. pp. 177–213.
620 https://doi.org/10.1007/978-1-4612-3532-3_4

621 Breusch, T., Pagan, A.R., Breusch, T., Pagan, A., 1979. A Simple Test for Heteroscedasticity
622 and Random Coefficient Variation. *Econometrica* 47, 1287–94.

623 Çelik, İ., Günal, H., Acar, M., Acir, N., Bereket Barut, Z., Budak, M., 2019. Strategic tillage may
624 sustain the benefits of long-term no-till in a Vertisol under Mediterranean climate. *Soil
625 Tillage Res.* 185, 17–28. <https://doi.org/10.1016/j.still.2018.08.015>

626 Chagas, C. da S., de Carvalho Junior, W., Bhering, S.B., Calderano Filho, B., 2016. Spatial
627 prediction of soil surface texture in a semiarid region using random forest and multiple
628 linear regressions. *Catena* 139, 232–240. <https://doi.org/10.1016/j.catena.2016.01.001>

629 Chen, S., Richer-de-Forges, A.C., Saby, N.P.A., Martin, M.P., Walter, C., Arrouays, D., 2018.
630 Building a pedotransfer function for soil bulk density on regional dataset and testing its
631 validity over a larger area. *Geoderma* 312, 52–63.
632 <https://doi.org/10.1016/j.geoderma.2017.10.009>

633 Chen, S., Xu, D., Li, S., Ji, W., Yang, M., Zhou, Y., Hu, B., Xu, H., Shi, Z., 2020. Monitoring
634 soil organic carbon in alpine soils using in situ vis-NIR spectroscopy and a multilayer
635 perceptron. *L. Degrad. Dev.* 31, 1026–1038. <https://doi.org/10.1002/ldr.3497>

636 Colombi, T., Torres, L.C., Walter, A., Keller, T., 2018. Feedbacks between soil penetration
637 resistance, root architecture and water uptake limit water accessibility and crop growth – A
638 vicious circle. *Sci. Total Environ.* 626, 1026–1035.
639 <https://doi.org/10.1016/j.scitotenv.2018.01.129>

640 de Souza, E., Fernandes Filho, E.I., Schaefer, C.E.G.R., Batjes, N.H., dos Santos, G.R., Pontes,

641 L.M., 2016. Pedotransfer functions to estimate bulk density from soil properties and
642 environmental covariates: Rio Doce basin. *Sci. Agric.* 73, 525–534.
643 <https://doi.org/10.1590/0103-9016-2015-0485>

644 De Vos, B., Van Meirvenne, M., Quataert, P., Deckers, J., Muys, B., 2005. Predictive quality of
645 pedotransfer functions for estimating bulk density of forest soils. *Soil Sci. Soc. Am. J.* 69,
646 500–510. <https://doi.org/10.2136/sssaj2005.0500>

647 Draper, N.R., Smith, H., 1998. *Applied Regression Analysis*, Third Edition, in:
648 DOI:10.1002/9781118625590 1998 John Wiley & Sons, Inc. pp. 1–704.

649 Ebrahimi, M., Sarikhani, M.R., Safari Sinangani, A.A., Ahmadi, A., Keesstra, S., 2019.
650 Estimating the soil respiration under different land uses using artificial neural network and
651 linear regression models. *Catena* 174, 371–382.
652 <https://doi.org/10.1016/j.catena.2018.11.035>

653 Evrendilek, F., Celik, I., Kilic, S., 2004. Changes in soil organic carbon and other physical soil
654 properties along adjacent Mediterranean forest, grassland, and cropland ecosystems in
655 Turkey. *J. Arid Environ.* 59, 743–752. <https://doi.org/10.1016/j.jaridenv.2004.03.002>

656 Farr, T.G., Rosen, P.A., Caro, E., Crippen, R., Duren, R., Hensley, S., Kobrick, M., Paller, M.,
657 Rodriguez, E., Roth, L., Seal, D., Shaffer, S., Shimada, J., Umland, J., Werner, M., Oskin,
658 M., Burbank, D., Alsdorf, D.E., 2007. The shuttle radar topography mission. *Rev. Geophys.*
659 45. <https://doi.org/10.1029/2005RG000183>

660 Fick, S.E., Hijmans, R.J., 2017. WorldClim 2: new 1-km spatial resolution climate surfaces for
661 global land areas. *Int. J. Climatol.* 37, 4302–4315. <https://doi.org/10.1002/joc.5086>

662 Fila, G., Bellocchi, G., Donatelli, M., Acutis, M., 2003. IRENE_DLL: A Class Library for
663 Evaluating Numerical Estimates. *Agron. J.* 95, 1330–1333.

664 <https://doi.org/10.2134/agronj2003.1330>

665 Fox, D.G., 1981. Judging Air Quality Model Performance. [https://doi.org/10.1175/1520-](https://doi.org/10.1175/1520-0477(1981)062<0599:JAQMP>2.0.CO;2)

666 [0477\(1981\)062<0599:JAQMP>2.0.CO;2](https://doi.org/10.1175/1520-0477(1981)062<0599:JAQMP>2.0.CO;2)

667 Francaviglia, R., Álvaro-Fuentes, J., Di Bene, C., Gai, L., Regina, K., Turtola, E., 2020.

668 Diversification and management practices in selected European regions. A data analysis of

669 arable crops production. *Agronomy* 10, 297. <https://doi.org/10.3390/agronomy10020297>

670 Ghani, I.M.M., Ahmad, S., 2010. Stepwise multiple regression method to forecast fish landing,

671 in: *Procedia - Social and Behavioral Sciences*. Elsevier Ltd, pp. 549–554.

672 <https://doi.org/10.1016/j.sbspro.2010.12.076>

673 Ghehi, N.G., Nemes, A., Verdoodt, A., Van Ranst, E., Cornelis, W.M., Boeckx, P., 2012.

674 Nonparametric Techniques for Predicting Soil Bulk Density of Tropical Rainforest Topsoils

675 in Rwanda. *Soil Sci. Soc. Am. J.* 76, 1172–1183. <https://doi.org/10.2136/sssaj2011.0330>

676 Gozubuyuk, Z., Sahin, U., Ozturk, I., Celik, A., Adiguzel, M.C., 2014. Tillage effects on certain

677 physical and hydraulic properties of a loamy soil under a crop rotation in a semi-arid region

678 with a cool climate. *Catena* 118, 195–205. <https://doi.org/10.1016/j.catena.2014.01.006>

679 Håkansson, I., Lipiec, J., 2000. A review of the usefulness of relative bulk density values in

680 studies of soil structure and compaction. *Soil Tillage Res.* [https://doi.org/10.1016/S0167-](https://doi.org/10.1016/S0167-1987(99)00095-1)

681 [1987\(99\)00095-1](https://doi.org/10.1016/S0167-1987(99)00095-1)

682 Hamilton, N.E., Ferry, M., 2018. Ggtern: Ternary diagrams using ggplot2. *J. Stat. Softw.* 87, 1–

683 17. <https://doi.org/10.18637/jss.v087.c03>

684 Haykin, S., 2008. *Neural Networks and Learning Machines*, Pearson Prentice Hall New Jersey

685 USA 936. <https://doi.org/978-0131471399>

686 Hengl, T., De Jesus, J.M., Heuvelink, G.B.M., Gonzalez, M.R., Kilibarda, M., Blagotić, A.,

687 Shangguan, W., Wright, M.N., Geng, X., Bauer-Marschallinger, B., Guevara, M.A., Vargas,
688 R., MacMillan, R.A., Batjes, N.H., Leenaars, J.G.B., Ribeiro, E., Wheeler, I., Mantel, S.,
689 Kempen, B., 2017. SoilGrids250m: Global gridded soil information based on machine
690 learning. *PLoS One* 12. <https://doi.org/10.1371/journal.pone.0169748>

691 Hiederer, R., Jones, R.J.A., Daroussin, J., 2006. Soil Profile Analytical Database for Europe
692 (SPADE): Reconstruction and validation of the measured data (SPADE/M). *Geogr. Tidsskr.*
693 106, 71–85. <https://doi.org/10.1080/00167223.2006.10649546>

694 Hollis, J.M., Hannam, J., Bellamy, P.H., 2012. Empirically-derived pedotransfer functions for
695 predicting bulk density in European soils. *Eur. J. Soil Sci.* 63, 96–109.
696 <https://doi.org/10.1111/j.1365-2389.2011.01412.x>

697 Khaledian, Y., Miller, B.A., 2020. Selecting appropriate machine learning methods for digital
698 soil mapping. *Appl. Math. Model.* 81, 401–418. <https://doi.org/10.1016/j.apm.2019.12.016>

699 Lagacherie, P., Álvaro-Fuentes, J., Annabi, M., Bernoux, M., Bouarfa, S., Douaoui, A.,
700 Grünberger, O., Hammani, A., Montanarella, L., Mrabet, R., Sabir, M., Raclot, D., 2018.
701 Managing Mediterranean soil resources under global change: expected trends and
702 mitigation strategies. *Reg. Environ. Chang.* 18, 663–675. [https://doi.org/10.1007/s10113-](https://doi.org/10.1007/s10113-017-1239-9)
703 [017-1239-9](https://doi.org/10.1007/s10113-017-1239-9)

704 Leij, F.J., Romano, N., Palladino, M., Schaap, M.G., Coppola, A., 2004. Topographical attributes
705 to predict soil hydraulic properties along a hillslope transect. *Water Resour. Res.* 40.
706 <https://doi.org/10.1029/2002WR001641>

707 Lionello, P., Malanotte-Rizzoli, P., Boscolo, R., Alpert, P., Artale, V., Li, L., Luterbacher, J.,
708 May, W., Trigo, R., Tsimplis, M., Ulbrich, U., Xoplaki, E., 2006. The Mediterranean
709 climate: An overview of the main characteristics and issues. *Dev. Earth Environ. Sci.*

710 [https://doi.org/10.1016/S1571-9197\(06\)80003-0](https://doi.org/10.1016/S1571-9197(06)80003-0)

711 Makovníková, J., Širáň, M., Houšková, B., Pálka, B., Jones, A., 2017. Comparison of different
712 models for predicting soil bulk density. Case study - Slovakian agricultural soils. *Int.*
713 *Agrophysics* 31, 491–498. <https://doi.org/10.1515/intag-2016-0079>

714 Manrique, L.A., Jones, C.A., 1991. Bulk density of soils in relation to soil physical and chemical
715 properties. *Soil Sci. Soc. Am. J.* 55, 476–481.
716 <https://doi.org/10.2136/sssaj1991.03615995005500020030x>

717 Martín, M.Á., Reyes, M., Taguas, F.J., 2017. Estimating soil bulk density with information
718 metrics of soil texture. *Geoderma* 287, 66–70.
719 <https://doi.org/10.1016/j.geoderma.2016.09.008>

720 Mazzoncini, M., Sapkota, T.B., Bàrberi, P., Antichi, D., Risaliti, R., Bahadur, T., Ba, P., 2011.
721 Long-term effect of tillage, nitrogen fertilization and cover crops on soil organic carbon and
722 total nitrogen content. *Soil Tillage Res.* 114, 165–174.
723 <https://doi.org/10.1016/j.still.2011.05.001>

724 Minasny, B., McBratney, A.B., 2002. The neuro-m method for fitting neural network parametric
725 pedotransfer functions. *Soil Sci. Soc. Am. J.* 66, 352–361.
726 <https://doi.org/10.2136/sssaj2002.3520>

727 Minasny, B., McBratney, A.B., Malone, B.P., Wheeler, I., 2013. Chapter One – Digital Mapping
728 of Soil Carbon, in: *Advances in Agronomy*. pp. 1–47. [https://doi.org/10.1016/B978-0-12-](https://doi.org/10.1016/B978-0-12-405942-9.00001-3)
729 [405942-9.00001-3](https://doi.org/10.1016/B978-0-12-405942-9.00001-3)

730 Montzka, C., Herbst, M., Weihermüller, L., Verhoef, A., Vereecken, H., 2017. A global data set
731 of soil hydraulic properties and sub-grid variability of soil water retention and hydraulic
732 conductivity curves. *Earth Syst. Sci. Data* 9, 529–543. <https://doi.org/10.5194/essd-9-529->

733 2017

734 Moriasi D., Arnold J. G., Van Liew M. W., Bingner R. L., Harmel R. D., Veith T. L., 2007.

735 Model Evaluation Guidelines for Systematic Quantification of Accuracy in Watershed

736 Simulations. *Trans. ASABE* 50, 885–900. <https://doi.org/10.13031/2013.23153>

737 Morin, K., Davis, J.L., 2017. Cross-validation: What is it and how is it used in regression?

738 *Commun. Stat. - Theory Methods* 46, 5238–5251.

739 <https://doi.org/10.1080/03610926.2015.1099672>

740 Nasta, P., Palladino, M., Sica, B., Pizzolante, A., Trifuoggi, M., Toscanesi, M., Giarra, A.,

741 D’Auria, J., Nicodemo, F., Mazzitelli, C., Lazzaro, U., Di Fiore, P., Romano, N., 2020.

742 Evaluating pedotransfer functions for predicting soil bulk density using hierarchical

743 mapping information in Campania, Italy. *Geoderma Reg.*

744 <https://doi.org/10.1016/j.geodrs.2020.e00267>

745 Noryani, M., Sapuan, S.M., Mastura, M.T., Zuhri, M.Y.M., Zainudin, E.S., 2019. Material

746 selection of natural fibre using a stepwise regression model with error analysis. *J. Mater.*

747 *Res. Technol.* 8, 2865–2879. <https://doi.org/10.1016/j.jmrt.2019.02.019>

748 Nussbaum, M., Spiess, K., Baltensweiler, A., Grob, U., Keller, A., Greiner, L., Schaepman,

749 M.E., Papritz, A., 2018. Evaluation of digital soil mapping approaches with large sets of

750 environmental covariates. *SOIL* 4, 1–22. <https://doi.org/10.5194/soil-4-1-2018>

751 Pachepsky, Y.A., Timlin, D., Varallyay, G., 1996. Artificial neural networks to estimate soil

752 water retention from easily measurable data. *Soil Sci. Soc. Am. J.* 60, 727–733.

753 <https://doi.org/10.2136/sssaj1996.03615995006000030007x>

754 Panagos, P., Hiederer, R., Van Liedekerke, M., Bampa, F., 2013. Estimating soil organic carbon

755 in Europe based on data collected through an European network. *Ecol. Indic.* 24, 439–450.

756 <https://doi.org/10.1016/j.ecolind.2012.07.020>

757 Patil, N.G., Singh, S.K., 2016. Pedotransfer Functions for Estimating Soil Hydraulic Properties:
758 A Review. *Pedosphere* 26, 417–430. [https://doi.org/10.1016/S1002-0160\(15\)60054-6](https://doi.org/10.1016/S1002-0160(15)60054-6)

759 Perego, A., Rocca, A., Cattivelli, V., Tabaglio, V., Fiorini, A., Barbieri, S., Schillaci, C.,
760 Chiodini, M.E., Brenna, S., Acutis, M., 2019. Agro-environmental aspects of conservation
761 agriculture compared to conventional systems: A 3-year experience on 20 farms in the Po
762 valley (Northern Italy). *Agric. Syst.* 168, 73–87. <https://doi.org/10.1016/j.agry.2018.10.008>

763 Pezzuolo, A., Dumont, B., Sartori, L., Marinello, F., De Antoni Migliorati, M., Basso, B., 2017.
764 Evaluating the impact of soil conservation measures on soil organic carbon at the farm
765 scale. *Comput. Electron. Agric.* 135, 175–182.
766 <https://doi.org/10.1016/j.compag.2017.02.004>

767 Picciafuoco, T., Morbidelli, R., Flammini, A., Saltalippi, C., Corradini, C., Strauss, P., Blöschl,
768 G., 2019. A pedotransfer function for field-scale saturated hydraulic conductivity of a small
769 watershed. *Vadose Zo. J.* 18. <https://doi.org/10.2136/vzj2019.02.0018>

770 Piñeiro, G., Perelman, S., Guerschman, J.P., Paruelo, J.M., 2008. How to evaluate models:
771 Observed vs. predicted or predicted vs. observed? *Ecol. Modell.* 216, 316–322.
772 <https://doi.org/10.1016/j.ecolmodel.2008.05.006>

773 Premrov, A., Cummins, T., Byrne, K.A., 2018. Bulk-density modelling using optimal power-
774 transformation of measured physical and chemical soil parameters. *Geoderma* 314, 205–
775 220. <https://doi.org/10.1016/j.geoderma.2017.10.060>

776 Ramcharan, A., Hengl, T., Beaudette, D., Wills, S., 2017. A soil bulk density pedotransfer
777 function based on machine learning: A case study with the ncss soil characterization
778 database. *Soil Sci. Soc. Am. J.* 81, 1279–1287. <https://doi.org/10.2136/sssaj2016.12.0421>

779 Rawls, W.J., 1983. Estimating soil bulk density from particle size analysis and organic matter
780 content. *Soil Sci.* <https://doi.org/10.1097/00010694-198302000-00007>

781 Rawls, W.J., Pachepsky, Y.A., 2002. Using field topographic descriptors to estimate soil water
782 retention. *Soil Sci.* 167, 423–435. <https://doi.org/10.1097/00010694-200207000-00001>

783 Reidy, B., Simo, I., Sills, P., Creamer, R.E., 2016. Pedotransfer functions for Irish soils
784 – estimation of bulk density (ρ_b) per horizon type. *SOIL* 2, 25–39.
785 <https://doi.org/10.5194/soil-2-25-2016>

786 Reynolds, C.A., Jackson, T.J., Rawls, W.J., 2000. Estimating soil water-holding capacities by
787 linking the Food and Agriculture Organization Soil map of the world with global pedon
788 databases and continuous pedotransfer functions. *Water Resour. Res.* 36, 3653–3662.
789 <https://doi.org/10.1029/2000WR900130>

790 Rodríguez-Lado, L., Rial, M., Taboada, T., Cortizas, A.M., 2015. A Pedotransfer Function to
791 Map Soil Bulk Density from Limited Data. *Procedia Environ. Sci.* 27, 45–48.
792 <https://doi.org/10.1016/j.proenv.2015.07.112>

793 Román Dobarco, M., Cousin, I., Le Bas, C., Martin, M.P., 2019. Pedotransfer functions for
794 predicting available water capacity in French soils, their applicability domain and associated
795 uncertainty. *Geoderma* 336, 81–95. <https://doi.org/10.1016/j.geoderma.2018.08.022>

796 Romano, N., Chirico, G.B., 2004. The role of terrain analysis in using and developing
797 pedotransfer functions. *Dev. Soil Sci.* [https://doi.org/10.1016/S0166-2481\(04\)30016-4](https://doi.org/10.1016/S0166-2481(04)30016-4)

798 Saxton, K.E., Rawls, W.J., Romberger, J.S., Papendick, R.I., 1986. Estimating generalized soil-
799 water characteristics from texture. *Soil Sci. Soc. Am. J.* 50, 1031–1036.
800 <https://doi.org/10.2136/sssaj1986.03615995005000040039x>

801 Schaap, M.G., Leij, F.J., Van Genuchten, M.T., 1998. Neural network analysis for hierarchical

802 prediction of soil hydraulic properties. *Soil Sci. Soc. Am. J.* 62, 847–855.
803 <https://doi.org/10.2136/sssaj1998.03615995006200040001x>

804 Schillaci, C., Acutis, M., Lombardo, L., Lipani, A., Fantappiè, M., Märker, M., Saia, S., 2017a.
805 Spatio-temporal topsoil organic carbon mapping of a semi-arid Mediterranean region: The
806 role of land use, soil texture, topographic indices and the influence of remote sensing data to
807 modelling. *Sci. Total Environ.* 601–602, 821–832.
808 <https://doi.org/10.1016/j.scitotenv.2017.05.239>

809 Schillaci, C., Acutis, M., Vesely, F., Saia, S., 2019. A simple pipeline for the assessment of
810 legacy soil datasets: An example and test with soil organic carbon from a highly variable
811 area. *Catena* 175, 110–122. <https://doi.org/10.1016/j.catena.2018.12.015>

812 Schillaci, C., Lombardo, L., Saia, S., Fantappiè, M., Märker, M., Acutis, M., 2017b. Modelling
813 the topsoil carbon stock of agricultural lands with the Stochastic Gradient Treeboost in a
814 semi-arid Mediterranean region. *Geoderma* 286, 35–45.
815 <https://doi.org/10.1016/j.geoderma.2016.10.019>

816 Schillaci, C., Saia, S., Acutis, M., 2018. Modelling of Soil Organic Carbon in the Mediterranean
817 area: a systematic map. *Rend. Online della Soc. Geol. Ital.* 4, 161–166.

818 Sequeira, C.H., Wills, S.A., Seybold, C.A., West, L.T., 2014. Predicting soil bulk density for
819 incomplete databases. *Geoderma* 213, 64–73.
820 <https://doi.org/10.1016/j.geoderma.2013.07.013>

821 Sevastas, S., Gasparatos, D., Botsis, D., Siarkos, I., Diamantaras, K.I., Bilas, G., 2018. Predicting
822 bulk density using pedotransfer functions for soils in the Upper Anthemountas basin,
823 Greece. *Geoderma Reg.* 14. <https://doi.org/10.1016/j.GEODRS.2018.e00169>

824 Tao, F., Palosuo, T., Valkama, E., Mäkipää, R., 2019. Cropland soils in China have a large

825 potential for carbon sequestration based on literature survey. *Soil Tillage Res.*
826 <https://doi.org/10.1016/j.still.2018.10.009>

827 Tejada, M., Hernandez, M.T., Garcia, C., 2009. Soil restoration using composted plant residues:
828 Effects on soil properties. *Soil Tillage Res.* 102, 109–117.
829 <https://doi.org/10.1016/j.still.2008.08.004>

830 Thompson, B., 2006. *Foundations of Behavioral Statistics*, pp 470. Guilford Publications.

831 Throop, H.L., Archer, S.R., Monger, H.C., Waltman, S., 2012. When bulk density methods
832 matter: Implications for estimating soil organic carbon pools in rocky soils. *J. Arid Environ.*
833 77, 66–71. <https://doi.org/10.1016/j.jaridenv.2011.08.020>

834 Tietje, O., Tapkenhinrichs, M., 1993. Evaluation of Pedo-Transfer Functions. *Soil Sci. Soc. Am.*
835 J. 57, 1088–1095. <https://doi.org/10.2136/sssaj1993.03615995005700040035x>

836 Tranter, G., Minasny, B., Mcbratney, A.B., Murphy, B., Mckenzie, N.J., Grundy, M., Brough,
837 D., 2007. Building and testing conceptual and empirical models for predicting soil bulk
838 density. *Soil Use Manag.* 23, 437–443. <https://doi.org/10.1111/j.1475-2743.2007.00092.x>

839 Valkama, E., Kunyapiyaeva, G., Zhapayev, R., Karabayev, M., Zhusupbekov, E., Perego, A.,
840 Schillaci, C., Sacco, D., Moretti, B., Grignani, C., Acutis, M., 2020. Can conservation
841 agriculture increase soil carbon sequestration? A modelling approach. *Geoderma* 369,
842 114298. <https://doi.org/10.1016/j.geoderma.2020.114298>

843 Van Looy, K., Bouma, J., Herbst, M., Koestel, J., Minasny, B., Mishra, U., Montzka, C., Nemes,
844 A., Pachepsky, Y.A., Padarian, J., Schaap, M.G., Tóth, B., Verhoef, A., Vanderborght, J.,
845 van der Ploeg, M.J., Weihermüller, L., Zacharias, S., Zhang, Y., Vereecken, H., 2017.
846 *Pedotransfer Functions in Earth System Science: Challenges and Perspectives*. *Rev.*
847 *Geophys.* <https://doi.org/10.1002/2017RG000581>

848 Verheye, W., De La Rosa, D., 2005. ©UNESCO-EOLSS Encyclopedia of Life Support Systems
849 Mediterranean Soils.

850 Veronesi, F., Schillaci, C., 2019. Comparison between geostatistical and machine learning
851 models as predictors of topsoil organic carbon with a focus on local uncertainty estimation.
852 *Ecol. Indic.* 101, 1032–1044. <https://doi.org/10.1016/j.ecolind.2019.02.026>

853 Wadoux, A.M.J.C., Samuel-Rosa, A., Poggio, L., Mulder, V.L., 2019. A note on knowledge
854 discovery and machine learning in digital soil mapping. *Eur. J. Soil Sci.*
855 <https://doi.org/10.1111/ejss.12909>

856 Wang, Y., Shao, M., Liu, Z., Zhang, C., 2014. Prediction of Bulk Density of Soils in the Loess
857 Plateau Region of China. *Surv. Geophys.* <https://doi.org/10.1007/s10712-013-9249-8>

858 Wösten, J.H.M., Lilly, A., Nemes, A., Le Bas, C., 1999. Development and use of a database of
859 hydraulic properties of European soils. *Geoderma* 90, 169–185.
860 [https://doi.org/10.1016/S0016-7061\(98\)00132-3](https://doi.org/10.1016/S0016-7061(98)00132-3)

861 Wösten, J.H.M., Verzandvoort, S.J.E., Leenaars, J.G.B., Hoogland, T., Wesseling, J.G., 2013.
862 Soil hydraulic information for river basin studies in semi-arid regions. *Geoderma* 195–196,
863 79–86. <https://doi.org/10.1016/j.geoderma.2012.11.021>

864 Xiangsheng, Y., Guosheng, L., Yanyu, Y., 2016. Pedotransfer Functions for Estimating Soil
865 Bulk Density: A Case Study in the Three-River Headwater Region of Qinghai Province,
866 China. *Pedosphere* 26, 362–373. [https://doi.org/10.1016/S1002-0160\(15\)60049-2](https://doi.org/10.1016/S1002-0160(15)60049-2)

867 Yaalon, D.H., 1997. Soils in the Mediterranean region: What makes them different? *Catena* 28,
868 157–169. [https://doi.org/10.1016/S0341-8162\(96\)00035-5](https://doi.org/10.1016/S0341-8162(96)00035-5)

869 Zdruli, P., Kapur, S., Çelik, I., 2011. Soils of the mediterranean region, their characteristics,
870 management and sustainable use, in: *Sustainable Land Management: Learning from the Past*

871 for the Future. Springer Berlin Heidelberg, pp. 125–142. <https://doi.org/10.1007/978-3-642->
872 14782-1_4

873 ----- REFERENCE FOR TAB 2 -----

- 874 Abou Zakhem, B., Al Ain, F., Hafez, R., 2019. Assessment of Field Water Budget Components
875 for Increasing Water Productivity Under Drip Irrigation in Arid and Semi-Arid Areas, Syria.
876 *Irrig. Drain.* 68, 452–463. <https://doi.org/10.1002/ird.2286>
- 877 Ali, S.A., Tedone, L., Verdini, L., Cazzato, E., De Mastro, G., 2019. Wheat response to no-tillage
878 and nitrogen fertilization in a long-term faba bean-based rotation. *Agronomy* 9, 50.
879 <https://doi.org/10.3390/agronomy9020050>
- 880 Álvaro-Fuentes, J., López, M. V., Cantero-Martinez, C., Arrúe, J.L., 2008. Tillage Effects on Soil
881 Organic Carbon Fractions in Mediterranean Dryland Agroecosystems. *Soil Sci. Soc. Am. J.*
882 72, 541–547. <https://doi.org/10.2136/sssaj2007.0164>
- 883 Antonopoulos, V.Z., Georgiou, P.E., Kolotouros, C.A., 2013. Soil water dynamics in cropped and
884 uncropped fields in northern Greece using a dual-permeability model. *Hydrol. Sci. J.* 58,
885 1748–1759. <https://doi.org/10.1080/02626667.2013.816424>
- 886 Bescansa, P., Imaz, M.J., Virto, I., Enrique, A., Hoogmoed, W.B., 2006. Soil water retention as
887 affected by tillage and residue management in semiarid Spain. *Soil Tillage Res.* 87, 19–27.
888 <https://doi.org/10.1016/j.still.2005.02.028>
- 889 Bogunovic, I., Pereira, P., Kisic, I., Sajko, K., Sraka, M., 2018. Tillage management impacts on
890 soil compaction, erosion and crop yield in Stagnosols (Croatia). *Catena* 160, 376–384.
891 <https://doi.org/10.1016/j.catena.2017.10.009>
- 892 Cardinael, R., Chevallier, T., Cambou, A., Béral, C., Barthès, B.G., Dupraz, C., Durand, C.,
893 Kouakoua, E., Chenu, C., 2017. Increased soil organic carbon stocks under agroforestry: A
894 survey of six different sites in France. *Agric. Ecosyst. Environ.* 236, 243–255.
895 <https://doi.org/10.1016/j.agee.2016.12.011>
- 896 Carozzi, M., Bregaglio, S., Scaglia, B., Bernardoni, E., Acutis, M., Confalonieri, R., 2013. The
897 development of a methodology using fuzzy logic to assess the performance of cropping
898 systems based on a case study of maize in the Po Valley. *Soil Use Manag.* 29, 576–585.
899 <https://doi.org/10.1111/sum.12066>
- 900 Çelik, İ., Günal, H., Acar, M., Acir, N., Bereket Barut, Z., Budak, M., 2019. Strategic tillage may
901 sustain the benefits of long-term no-till in a Vertisol under Mediterranean climate. *Soil*
902 *Tillage Res.* 185, 17–28. <https://doi.org/10.1016/j.still.2018.08.015>
- 903 Ceotto, E., Marchetti, R., Castelli, F., 2018. Residual soil nitrate as affected by giant reed
904 cultivation and cattle slurry fertilisation. *Ital. J. Agron.* 13, 317–323.
905 <https://doi.org/10.4081/ija.2018.1264>
- 906 Chennafi, H., Aïdaoui, A., Bouzerzour, H., Saci, A., 2006. Yield response of durum wheat
907 (*Triticum durum* Desf.) cultivar Waha to deficit irrigation under semi arid growth conditions.

908 Asian J. Plant Sci. 5, 854–860. <https://doi.org/10.3923/ajps.2006.854.860>

909 Diacono, M., Ciaccia, C., Canali, S., Fiore, A., Montemurro, F., 2018. Assessment of agro-
910 ecological service crop managements combined with organic fertilisation strategies in organic
911 melon crop. *Ital. J. Agron.* 13, 172–182. <https://doi.org/10.4081/ija.2018.951>

912 Jemai, I., Ben Aissa, N., Ben Guirat, S., Ben-Hammouda, M., Gallali, T., 2013. Impact of three
913 and seven years of no-tillage on the soil water storage, in the plant root zone, under a dry
914 subhumid Tunisian climate. *Soil Tillage Res.* 126, 26–33.
915 <https://doi.org/10.1016/j.still.2012.07.008>

916 Kargas, G., Kerkides, P., Poulouvassilis, A., 2012. Infiltration of rain water in semi-arid areas under
917 three land surface treatments. *Soil Tillage Res.* 120, 15–24.
918 <https://doi.org/10.1016/j.still.2012.01.004>

919 Mahmoud, E., Ibrahim, M., Abd El-Rahman, L., Khader, A., 2019. Effects of Biochar and
920 Phosphorus Fertilizers on Phosphorus Fractions, Wheat Yield and Microbial Biomass Carbon
921 in Vertic Torrifluvents. *Commun. Soil Sci. Plant Anal.* 50, 362–372.
922 <https://doi.org/10.1080/00103624.2018.1563103>

923 Marquez-Garcia, F., Gonzalez-Sanchez, E.J., Castro-Garcia, S., Ordoñez-Fernandez, R., 2013.
924 Improvement of soil carbon sink by cover crops in olive orchards under semiarid conditions.
925 Influence of the type of soil and weed. *Spanish J. Agric. Res.* 11, 335–346.
926 <https://doi.org/10.5424/sjar/2013112-3558>

927 Muñoz-Rojas, M., Doro, L., Ledda, L., Francaviglia, R., 2015. Application of CarboSOIL model
928 to predict the effects of climate change on soil organic carbon stocks in agro-silvo-pastoral
929 Mediterranean management systems. *Agric. Ecosyst. Environ.* 202, 8–16.
930 <https://doi.org/10.1016/j.agee.2014.12.014>

931 Ozpinar, S., Ozpinar, A., Cay, A., 2018. Soil management effect on soil properties in traditional
932 and mechanized vineyards under a semiarid Mediterranean environment. *Soil Tillage Res.*
933 178, 198–208. <https://doi.org/10.1016/j.still.2018.01.004>

934 Pardo, J.J., Martínez-Romero, A., Lélis, B.C., Tarjuelo, J.M., Domínguez, A., 2020. Effect of the
935 optimized regulated deficit irrigation methodology on water use in barley under semiarid
936 conditions. *Agric. Water Manag.* 228, 105925. <https://doi.org/10.1016/j.agwat.2019.105925>

937 Pareja-Sánchez, E., Plaza-Bonilla, D., Ramos, M.C., Lampurlanés, J., Álvaro-Fuentes, J., Cantero-
938 Martínez, C., 2017. Long-term no-till as a means to maintain soil surface structure in an
939 agroecosystem transformed into irrigation. *Soil Tillage Res.* 174, 221–230.
940 <https://doi.org/10.1016/j.still.2017.07.012>

941 Perego, A., Rocca, A., Cattivelli, V., Tabaglio, V., Fiorini, A., Barbieri, S., Schillaci, C., Chiodini,
942 M.E., Brenna, S., Acutis, M., 2019. Agro-environmental aspects of conservation agriculture
943 compared to conventional systems: A 3-year experience on 20 farms in the Po valley
944 (Northern Italy). *Agric. Syst.* 168, 73–87. <https://doi.org/10.1016/j.agsy.2018.10.008>

945 Pezzuolo, A., Dumont, B., Sartori, L., Marinello, F., De Antoni Migliorati, M., Basso, B., 2017.
946 Evaluating the impact of soil conservation measures on soil organic carbon at the farm scale.

947 Comput. Electron. Agric. 135, 175–182. <https://doi.org/10.1016/j.compag.2017.02.004>
948 Recio, J., Vallejo, A., Le-Noë, J., Garnier, J., García-Marco, S., Álvarez, J.M., Sanz-Cobena, A.,
949 2018. The effect of nitrification inhibitors on NH₃ and N₂O emissions in highly N fertilized
950 irrigated Mediterranean cropping systems. *Sci. Total Environ.* 636, 427–436.
951 <https://doi.org/10.1016/j.scitotenv.2018.04.294>
952 Stavi, I., Ungar, E.D., Lavee, H., Sarah, P., 2008. Grazing-induced spatial variability of soil bulk
953 density and content of moisture, organic carbon and calcium carbonate in a semi-arid
954 rangeland. *Catena* 75, 288–296. <https://doi.org/10.1016/j.catena.2008.07.007>
955 Tolon-Becerra, A., Tourn, M., Botta, G.F., Lastra-Bravo, X., 2011. Effects of different tillage
956 regimes on soil compaction, maize (*Zea mays* L.) seedling emergence and yields in the eastern
957 Argentinean Pampas region. *Soil Tillage Res.* 117, 184–190.
958 <https://doi.org/10.1016/j.still.2011.10.003>
959 Valboa, G., Lagomarsino, A., Brandi, G., Agnelli, A.E., Simoncini, S., Papini, R., Vignozzi, N.,
960 Pellegrini, S., 2015. Long-term variations in soil organic matter under different tillage
961 intensities. *Soil Tillage Res.* 154, 126–135. <https://doi.org/10.1016/j.still.2015.06.017>
962 Visconti, F., Salvador, A., Navarro, P., de Paz, J.M., 2019. Effects of three irrigation systems on
963 ‘Piel de sapo’ melon yield and quality under salinity conditions. *Agric. Water Manag.* 226.
964 <https://doi.org/10.1016/j.agwat.2019.105829>
965 Vitale, L., Polimeno, F., Ottaiano, L., Maglione, G., Tedeschi, A., Mori, M., De Marco, A., Di
966 Tommasi, P., Magliulo, V., 2017. Fertilizer type influences tomato yield and soil N₂O
967 emissions. *Plant, Soil Environ.* 63, 105–110. <https://doi.org/10.17221/678/2016-PSE>
968 Zohry, A., Ouda, S., Hamd-alla, W., Shalaby, E.-S., 2017. Evaluation of different crop sequences
969 for wheat and maize in sandy soil. <https://doi.org/10.14720/aas.2017.109.2.21>
970